



3 1176 00161 4735

NASA CR-165131

NASA-CR-165131

1980 00 23716

NASA CR-165131



INTERACTION OF HIGH VOLTAGE
SURFACES WITH THE SPACE PLASMA

Prepared for
LEWIS RESEARCH CENTER
NATIONAL AERONAUTICS AND SPACE ADMINISTRATION
GRANT NSG 3196

LIBRARY COPY

OCT 7 1980

LANGLEY RESEARCH CENTER
LIBRARY, NASA
HAMPTON, VIRGINIA

Annual Report

May 1980

Harold R. Kaufman and Raymond S. Robinson
Department of Physics
Colorado State University
Fort Collins, Colorado



NF02428

1 Report No CR-165131	2 Government Accession No	3 Recipient's Catalog No	
4 Title and Subtitle Interaction of high voltage surfaces with the space plasma		5 Report Date May 1980	
		6 Performing Organization Code	
7 Author(s) Harold R. Kaufman and Raymond S. Robinson		8 Performing Organization Report No	
9 Performing Organization Name and Address Department of Physics Colorado State University Fort Collins, CO 80523		10 Work Unit No	
		11 Contract or Grant No NSG-3196	
12 Sponsoring Agency Name and Address National Aeronautics and Space Administration Washington, D.C. 20546		13 Type of Report and Period Covered Contractor Report	
		14 Sponsoring Agency Code	
15 Supplementary Notes Grant Manager: Norman T. Grier NASA Lewis Research Center Cleveland, Ohio 44135			
16 Abstract High voltage solar arrays are desired to provide spacecraft power while optimizing mass and power efficiency. Operating such arrays in the space plasma environment can result in anomalously large currents being collected through insulation defects. The understanding of this phenomenon is the objective of this research program. Polyimide (Kapton) was the insulating material used in all tests reported herein. Two thicknesses of polyimide were tested, with no effect found due to insulator thickness. In these tests the polyimide thickness was always much less than the pinhole diameter. The pinhole area was varied over an area range of more than 30:1. It was found that the current collected was independent of the pinhole area for hole diameters from 0.35 to 2.0 mm. Two types of adhesives were tried in two different configurations. The adhesives were chosen for their extreme difference in vacuum qualifications. Neither adhesive types nor configuration made a significant difference in current collection. The temperature of the insulating material was also varied. It was found that current collection decreased with increasing temperature and that the strength of the temperature dependence increased with increasing conductor potential. This effect may be associated with secondary electron emission from the surface of the polyimide. Tests were conducted to see if pinhole current collection decreased with time, as was indicated by the effects of several short tests. Current was collected for over four hours while the conductor potential was held constant at 1000 volts. A smooth decrease with time was not observed, but rather a roughly constant current collection with brief surges to high values. Tests were also conducted with the simulated solar cell biased negative. These tests were done only for low voltages (<1000 volts). The currents collected were of the magnitude expected from electrostatic probe theory. The current was found to be proportional to pinhole area.			
17 Key Words (Suggested by Author(s)) Plasma Physics Space Plasma Solar Arrays		18 Distribution Statement Unclassified-Unlimited	
19 Security Classif (of this report) Unclassified	20 Security Classif (of this page) Unclassified	21 No of Pages	22 Price*

* For sale by the National Technical Information Service, Springfield, Virginia 22161

This Page Intentionally Left Blank

TABLE OF CONTENTS

	<u>Page</u>
I. INTRODUCTION.....	1
II. APPARATUS AND PROCEDURE.....	3
Vacuum Facility.....	3
Solar Array Simulation.....	3
Procedure.....	6
III. EXPERIMENTAL RESULTS.....	7
Positive Bias - Electron Collection.....	7
Normalization.....	7
Verification of Experimental Procedure.....	7
Effect of Adhesive.....	9
Effect of Temperature.....	13
Variation of Current Collection with Time.....	17
Effect of Pinhole Size.....	19
Effect of Insulator Thickness.....	23
High Current Measurements.....	30
Negative Bias - Ion Collection.....	33
Normalization.....	33
Effect of Pinhole Size.....	34
Comparison with Planar Probe Theory.....	34
IV. CONCLUDING REMARKS.....	39
V. APPENDIX.....	41
VI. REFERENCES.....	44

LIST OF FIGURES

	<u>Page</u>
Fig. 2-1. Sketch of 45-cm vacuum chamber with sample holder (simulated solar cell) and hollow cathode for plasma generation.....	4
Fig. 2-2. Detailed sketch of sample holder (simulated solar cell).....	5
Fig. 3-1. Comparison of experimental electron collection data with two theories.....	8
Fig. 3-2. Effect of adhesive type and conductor temperature on electron collection, with adhesive covering entire conductor except under pinhole.....	10
Fig. 3-3. Effect of adhesive type and conductor temperature on electron collection, with adhesive covering entire conductor except for 1 cm ² area near pinhole...	11
Fig. 3-4. The effect of conductor temperature on electron collection.....	14
Fig. 3-5. Data of Fig. 3-4 plotted to show the effect of conductor temperature at constant conductor voltages..	15
Fig. 3-6. Power of temperature variation for electron current as a function of conductor potential.....	16
Fig. 3-7. Variation of electron current collection with collection time.....	18
Fig. 3-8. Effect of current collection on insulator appearance.....	20
Fig. 3-9. Electron current collection characteristics for a range of hole sizes in 0.051 mm thick polyimide, normalized by I_0	21
Fig. 3-10. Electron current collection characteristics for a range of hole sizes in 0.127 mm thick polyimide, normalized by I_0	22
Fig. 3-11. Electron current collection characteristics for a range of hole sizes in 0.051 mm thick polyimide, normalized by j_0	24
Fig. 3-12. Electron current collection characteristics for a range of hole sizes in 0.127 mm thick polyimide normalized by j_0	25

Fig. 3-13.	Electron current collection characteristics for two insulation thicknesses and a hole diameter of 0.35 mm normalized by j_o	26
Fig. 3-14.	Electron current collection characteristics for two insulation thicknesses and a hole diameter of 0.52 mm, normalized by j_o	27
Fig. 3-15.	Electron current collection characteristics for two insulation thicknesses and a hole diameter of 1.0 mm, normalized by j_o	28
Fig. 3-16.	Electron current collection characteristics for two insulation thicknesses and a hole diameter of 2.0 mm, normalized by j_o	29
Fig. 3-17.	Electron current collection characteristics extended to higher currents, normalized by j_o	31
Fig. 3-18.	Glow observed near pinhole at higher electron collected currents.....	32
Fig. 3-19.	Ion current collection characteristics for a range of hole sizes, normalized by j_{Bohm}	35
Fig. 3-20.	Ion current collection characteristics for a range of hole sizes, normalized by I_{Bohm}	36
Fig. 3-21.	Comparison of experimental ion current collection characteristics with planar probe theory.....	37
Fig. A-1.	Geometry of planar probe.....	42

I. INTRODUCTION

Solar cell arrays constitute the major source of reliable long-term power for spacecraft orbiting the earth operating in the near-earth environment. The minimization of total mass for such spacecraft results in the general requirement for high voltage solar arrays. The space plasma environment,¹⁻³ though, can result in large currents being collected by exposed solar cells, with corresponding reductions in power output from the array. A protective covering of transparent insulation is not a complete solution to the current collection problem, due to the expectation of defects, either from the various fabrication processes or from collisions with micrometeoroids.

Early experiments showed that positive electrodes behind pinhole openings in insulating sheets could collect electron currents far in excess of what would be expected from electrostatic probe theory.⁴ Subsequent experiments not only verified these large currents, but showed a wide range of results, depending on materials, configuration, and operating conditions used in the tests.⁵⁻⁸

The major objective of this research is to investigate the phenomenon of unexpectedly large leakage currents collected by small exposed areas of high voltage solar arrays operating in the plasma environment simulating space. This report covers the progress since the last annual report.⁹ The results of the last annual report are reviewed briefly below, and were restricted to positive biases relative to the plasma.

At the $10^5/\text{cm}^3$ plasma density range investigated, the effects of surface area surrounding the hole appeared to be limited to roughly

1 cm from the hole. Scribing the exposed surface of a polyimide (Kapton) insulator reduced the electron current collected by a factor of several, as did also the application of a 2×2 cm conducting grid on the surface of the polyimide.

The electron current collected was found to generally decrease with successive tests. For polyimide insulation, this current decrease was associated with a smoothing of the inside of the insulator hole. For glass insulation, the current reduction was associated with the deposition of an insulating layer on the conductor behind the hole.

A general conclusion, made from a variety of observations, was that the generation of a vapor from the insulation was a major factor in the current collection process.

The research done during the present support period involved only one type of insulating material, polyimide (Kapton). The parameters tested were: pinhole area, adhesive type and configuration, temperature, polyimide thickness, and the variation of current collection with time. Most of the tests involved a positive bias relative to the plasma, but some preliminary work was done with negative bias.

II. APPARATUS AND PROCEDURE

R. P. Stillwell

Vacuum Facility

The experiments were conducted in a 45 cm diameter bell jar. An argon hollow cathode was used as the source of the plasma in the bell jar facility. As indicated in Fig. 2-1, the hollow cathode was centrally located and directed toward the side of the bell jar. The only source of argon gas in the bell jar was the flow through the hollow cathode.

The hollow cathode and anode configuration differs from the configuration previously used.¹ The hollow cathode and anode were mounted horizontally so that the conical baffle previously capping the perforated anode could be removed in an attempt to increase plasma density without, at the same time, permitting a direct flow path of particles from the cathode to the sample. (The purpose of the baffle in the vertical orientation was to prevent such a direct path.)

Changing the cathode/anode configuration did not increase the plasma density, but did indicate that there was no direct interaction between the hollow cathode and sample, as the results did not change with configurations. On the other hand, operation with a vertical hollow cathode and no baffle did produce results that differed from those obtained with a baffle.

The measurements of the plasma characteristics were taken with a spherical Langmuir probe. The measurement techniques are described in detail in the previous report.¹

Solar Array Simulation

To both control and measure the effects of temperature, a new sample holder was fabricated (see Fig. 2-2). The sample holder was an

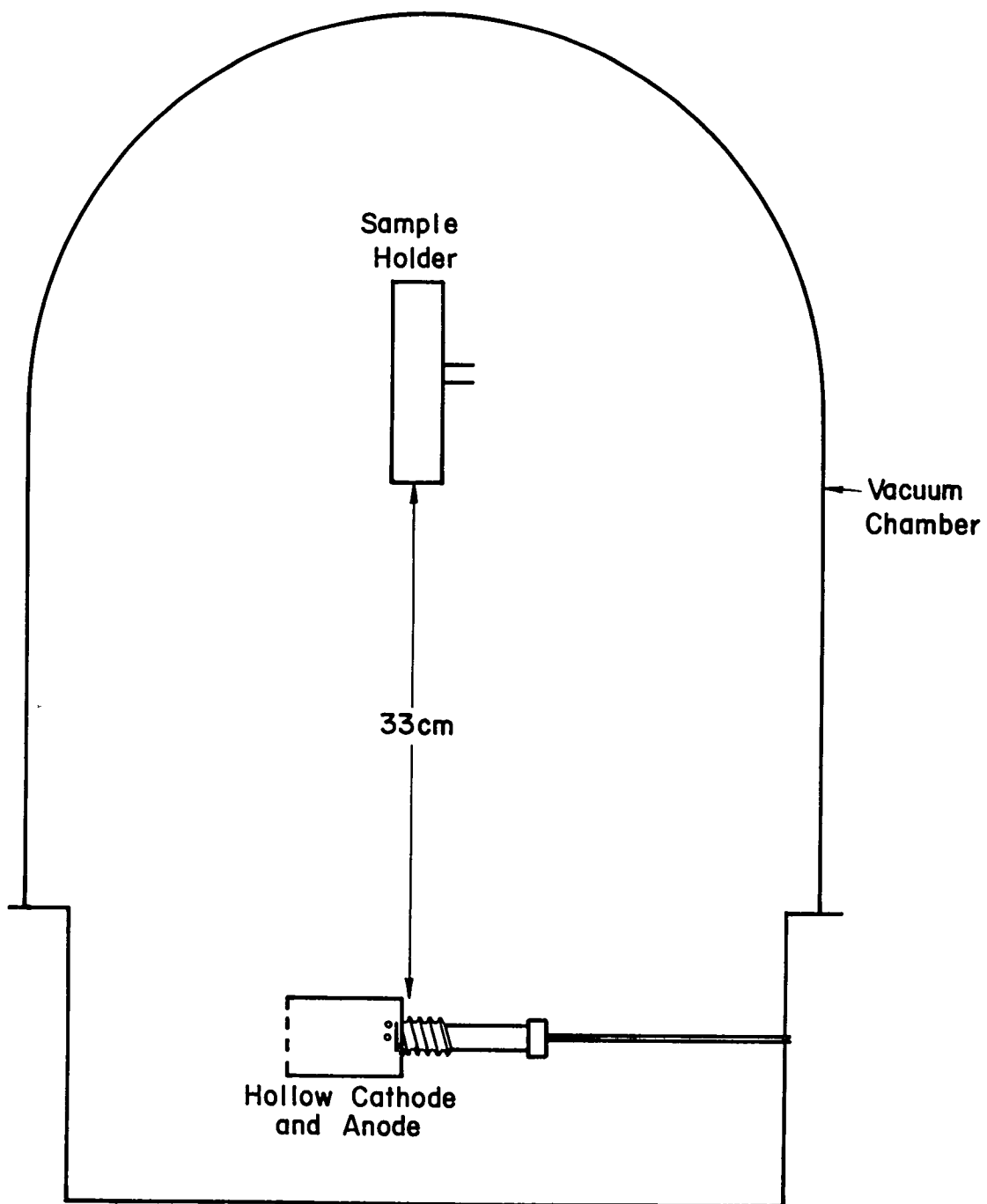


Fig. 2-1. Sketch of 45-cm vacuum chamber with sample holder (simulated solar cell) and hollow cathode for plasma generation.

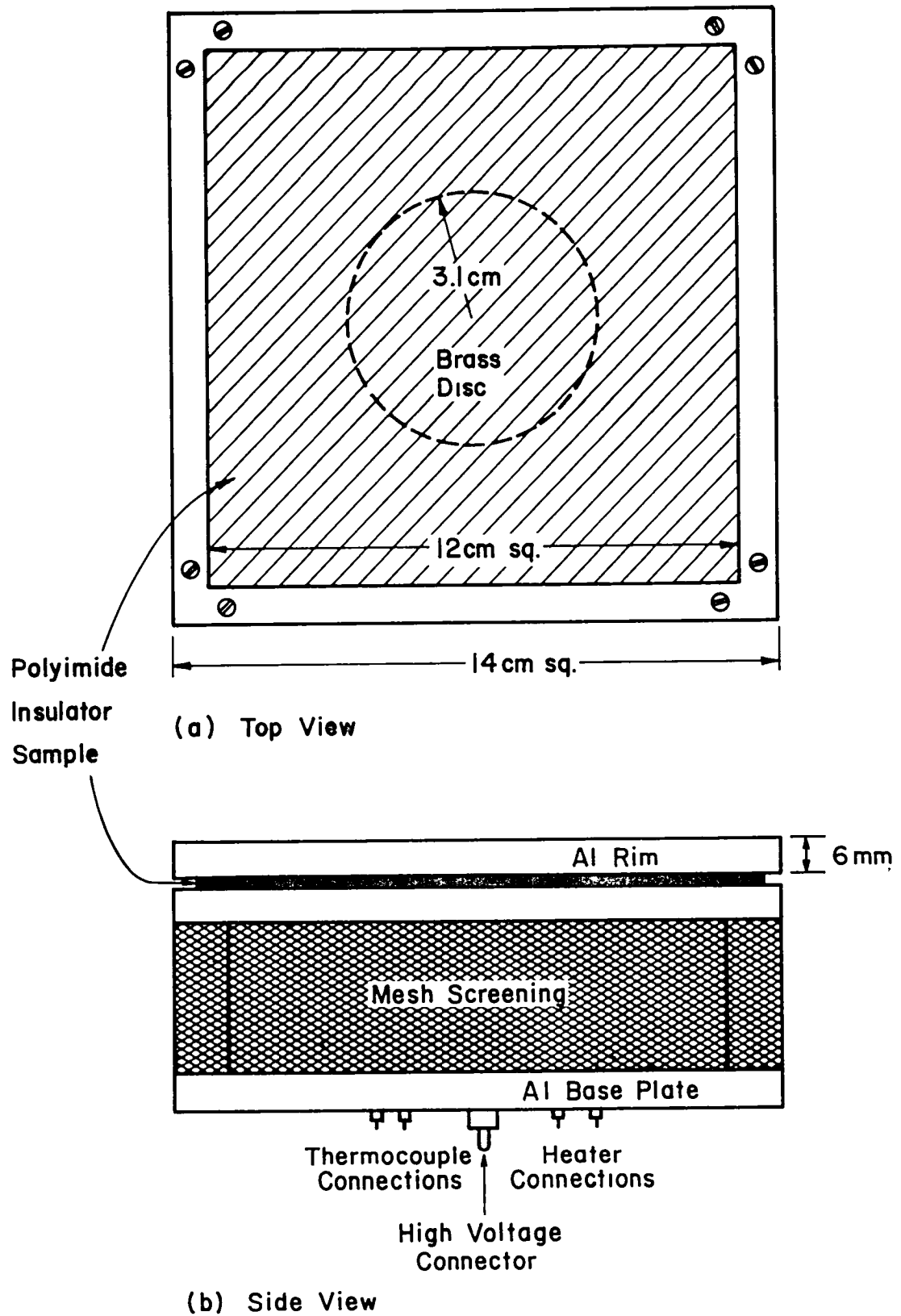


Fig. 2-2. Detailed sketch of sample holder (simulated solar cell).

aluminum frame containing a brass disc which simulated the solar cell. The brass disc (conductor) was insulated from the frame and protected from the plasma by a screen covering the aluminum frame. A baffle constructed of sheet metal was later placed over the screen to further isolate the interior of the holder.

The sample (an insulating film of polyimide) was placed between two aluminum rims, insulated from the aluminum by teflon film and attached with an adhesive to the conductor. A pinhole of known diameter was placed in the polyimide film, representing a defect in the insulator covering the solar cell.

A heater and thermocouple were attached to the brass disc. These permitted the control and measurement of the conductor temperature.

Procedure

The solar cell models were centrally and vertically mounted in the evacuated bell jar (see Fig. 2-1). A plasma of the desired density was generated and the temperature of the sample was adjusted to the desired setting. A slowly increasing voltage was then applied to the conductor causing current to be extracted from the plasma through the pinhole in the polyimide. The resulting current variation with voltage was recorded with a single test typically having a duration of several minutes. Langmuir probe traces were taken for measurement of plasma properties for each current-voltage test. Test variables included: pinhole area, polyimide thickness, temperature, adhesive type, adhesive configuration, and voltage polarity.

III. EXPERIMENTAL RESULTS

R. P. Stillwell

Positive Bias-Electron Collection

Normalization. The current/voltage data has been normalized by dividing the pinhole current by the random current,¹

$$I_o = \frac{1}{4} e n A_p \sqrt{\frac{8kT_e}{\pi m_e}} \quad (3-1)$$

where A_p is the area of conductor exposed by the pinhole, e is the magnitude of the electronic charge, n is the electron density, k is Boltzmann's constant, T_e is the electron temperature, and m_e is the electronic mass. All values are in SI units, unless otherwise specified. This normalization has been successfully used to eliminate scatter in the data due to electron density and temperature differences in the plasma environments of different tests.²

Correlation factors involving powers of the conductor potential were also tried. None of these correlations have, to date, yielded results that appear to be physically significant.

Verification of Experimental Procedure. Tests described in the previous annual report² were conducted to verify planar probe theory. These tests used the same experimental approach, except that a conducting surface at approximately ground potential replaced the insulator around the high potential conductor. The planar probe theory current-voltage curve, assuming a Maxwellian electron temperature, is indicated in Fig. 3-1.

With an insulator surrounding the high potential conductor, one would not, of course, expect exact agreement with planar probe theory. Another theory that might be expected to come closer to the use of a surrounding insulator is that of spherical probes - also shown in Fig. 3-1. When data using an insulator surrounding the high potential conductor are examined, though, the currents at a given voltage can be factors of 10 higher than either theory (again see Fig. 3-1).

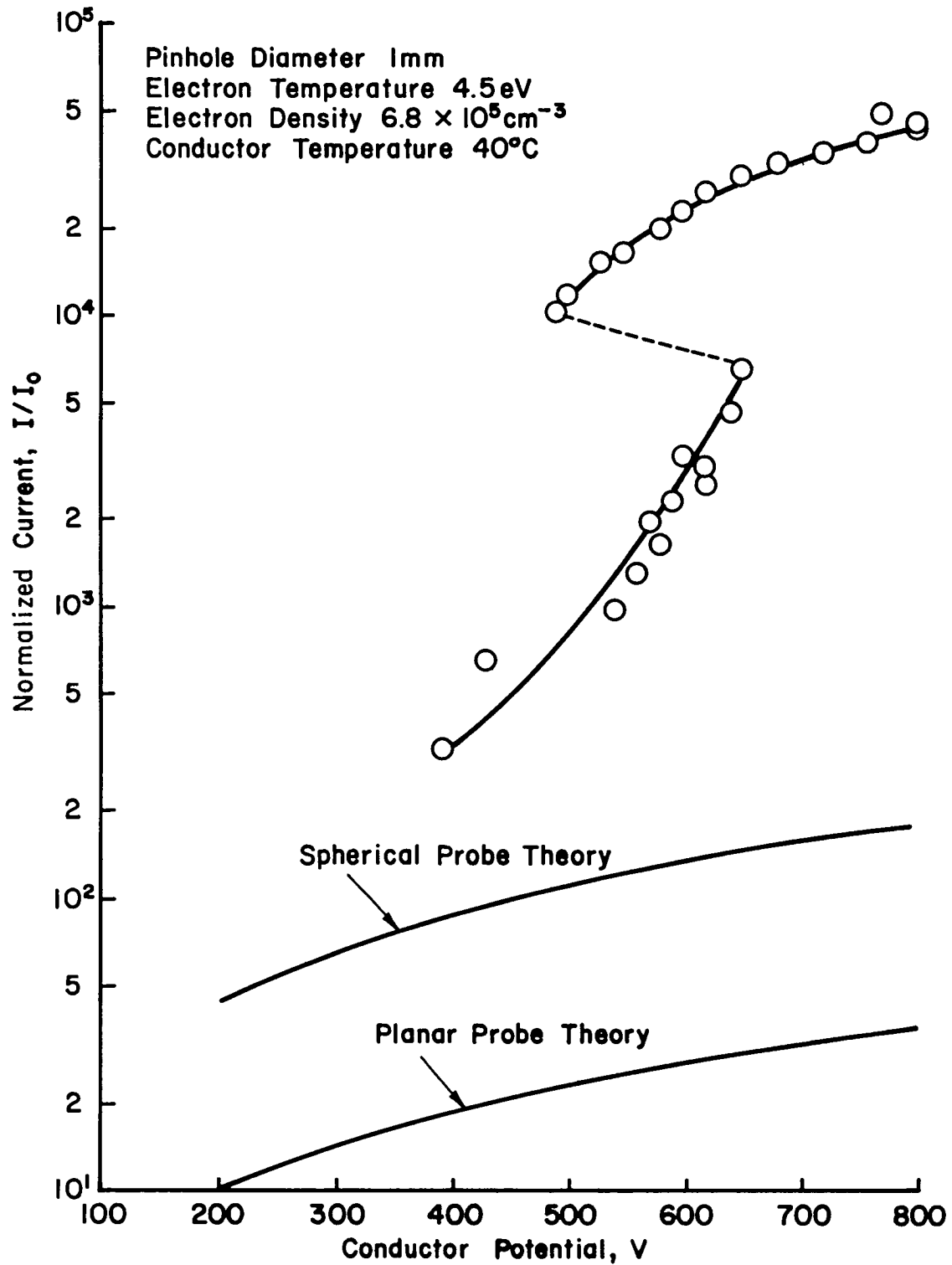


Fig. 3-1. Comparison of experimental electron collection data with two theories.

From Fig. 3-1, then, we conclude that planar and spherical probe theories differ by only a factor of several. Further, as mentioned above, planar probe theory was experimentally verified using the same experimental approach. The large increase in current using a surrounding insulator thus strongly indicates that the insulator has a strong enhancing effect on current collection.

Effect of Adhesive. Two types of double-sided pressure-sensitive adhesive sheets were tested, a low priced commercial brand (Scotch Double Stick Tape, by 3M) and a space qualified type (Y966, also by 3M). The low priced commercial adhesive was found to have modified sticking properties after testing at the higher temperatures, while no such change was evident for the space qualified adhesive. Such a change in properties for an organic material in a vacuum environment is almost always associated with outgassing. The two adhesives should thus have given substantially different results, if current collection were dependent on outgassing.

As a further check, these two different adhesives were tested in two different configurations. In one configuration the adhesive covered the entire conductor, except under the pinhole (Fig. 3-2). In the other configuration a 1 cm^2 area near the pinhole was left free of adhesive (Fig. 3-3).

In comparing Figs. 3-2 and 3-3, the adhesive configuration is not seen to be important. Also, there is no significant difference between the two adhesive types. Although the data are not shown, a test without adhesive also gave similar results to those shown in Figs. 3-2 and 3-3. (There was more scatter in the data obtained without adhesive, but this was believed due to thermal warping of the insulator sheet near the hole, causing changes in conductor to insulator distance.) Finally, the

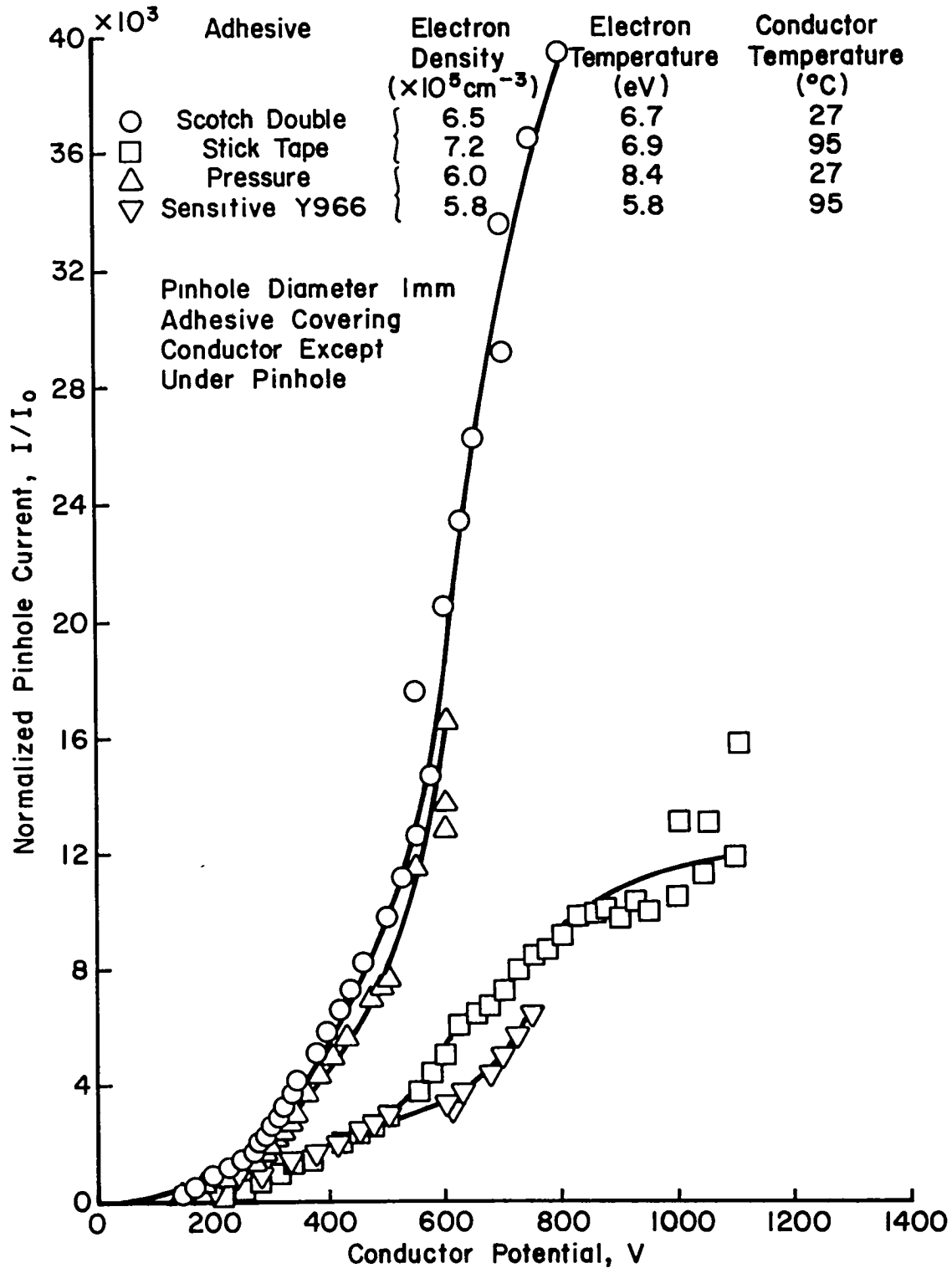


Fig. 3-2. Effect of adhesive type and conductor temperature on electron collection, with adhesive covering entire conductor except under pinhole.

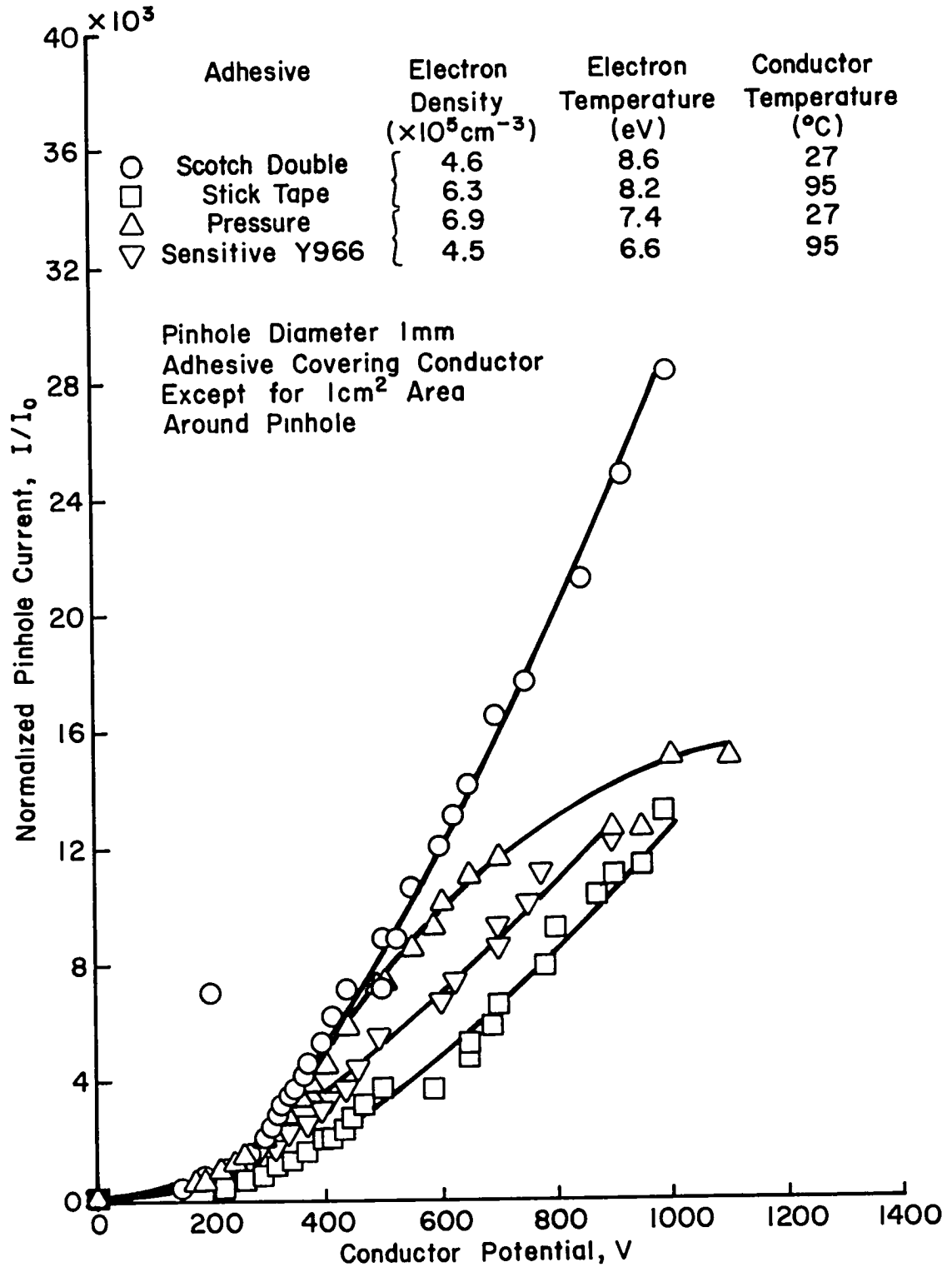


Fig. 3-3. Effect of adhesive type and conductor temperature on electron collection, with adhesive covering entire conductor except for 1 cm² area near pinhole.

current collected decreased with an increasing temperature. All of the above observations are consistent with thermally generated vapor not being important in the electron collection process.

In the previous annual report it was concluded that the generation of vapor was an important part of the process, due to observations of both deposition of insulator on the conductor and the large effect of surface texture within the hole. It appears clear from these earlier tests that some of the insulator can be vaporized by electron bombardment. The vapor generated by such bombardment should not be any more effective than a thermally generated vapor in augmenting electron collection. The significance of any vaporization by electron bombardment, then, appears to be in the deposition of that vapor on the conductor or in the modification of the insulator surface. This conclusion must, of course, be restricted to an operating condition with no visible glow near the pinhole. Visible glows were observed at higher collection currents, and will be discussed in a later section of this report.

For standardization of tests and better comparability of results, all subsequent tests described in this report used the space-qualified adhesive (Y966) with the adhesive covering the entire conductor except that area exposed by the pinhole. From an ideal viewpoint, it would be desirable to have only a conductor and an insulator present - with no adhesive between them. There is, however, the practical advantage of the adhesive preventing the occasional thermal buckling of the insulator that took place in its absence, as well as providing better thermal contact between insulator and conductor. Also, no adverse effect has been identified with the presence of the adhesive.

Effect of Temperature. A temperature effect on electron collection was noted in the preceding section. This effect will be examined in more detail in this section.

For the tests reported here, the conductor was heated to the desired temperature, in vacuum, for at least one hour before the application of high voltage. This procedure avoided the rapid outgassing that can accompany the heating of a surface in vacuum, as well as assuring thermal equilibrium of the insulator with the conductor. Five conductor temperatures were tested, from 27 to 120°C.

Data obtained at the five conductor temperatures are shown in Fig. 3-4. These data show a systematic decrease in collected electron current with increasing conductor (and insulator) temperature. The temperature variation of collected current is also shown in Fig. 3-5, which was obtained by crossplotting the faired curves of Fig. 3-4 for constant conductor voltages. The best fits for exponential variation of current with temperature are tabulated in Fig. 3-5 and shown graphically in Fig. 3-6. As shown clearly in Fig. 3-6, the absolute magnitude of the best fit temperature exponent increases with conductor voltage.

A model for the temperature variation of collected current is available from secondary electron emission. For insulators, secondary electron emission can have a temperature variation of $T^{-1/2.5}$. With the probability of a single secondary electron emission event varying as $T^{-1/2}$, the large negative powers in Fig. 3-6 can be inferred as resulting from a number of secondary electron events in series. Further, the larger negative powers at higher conductor voltages seem to indicate that the number of serial secondary electron events increases with conductor voltage.

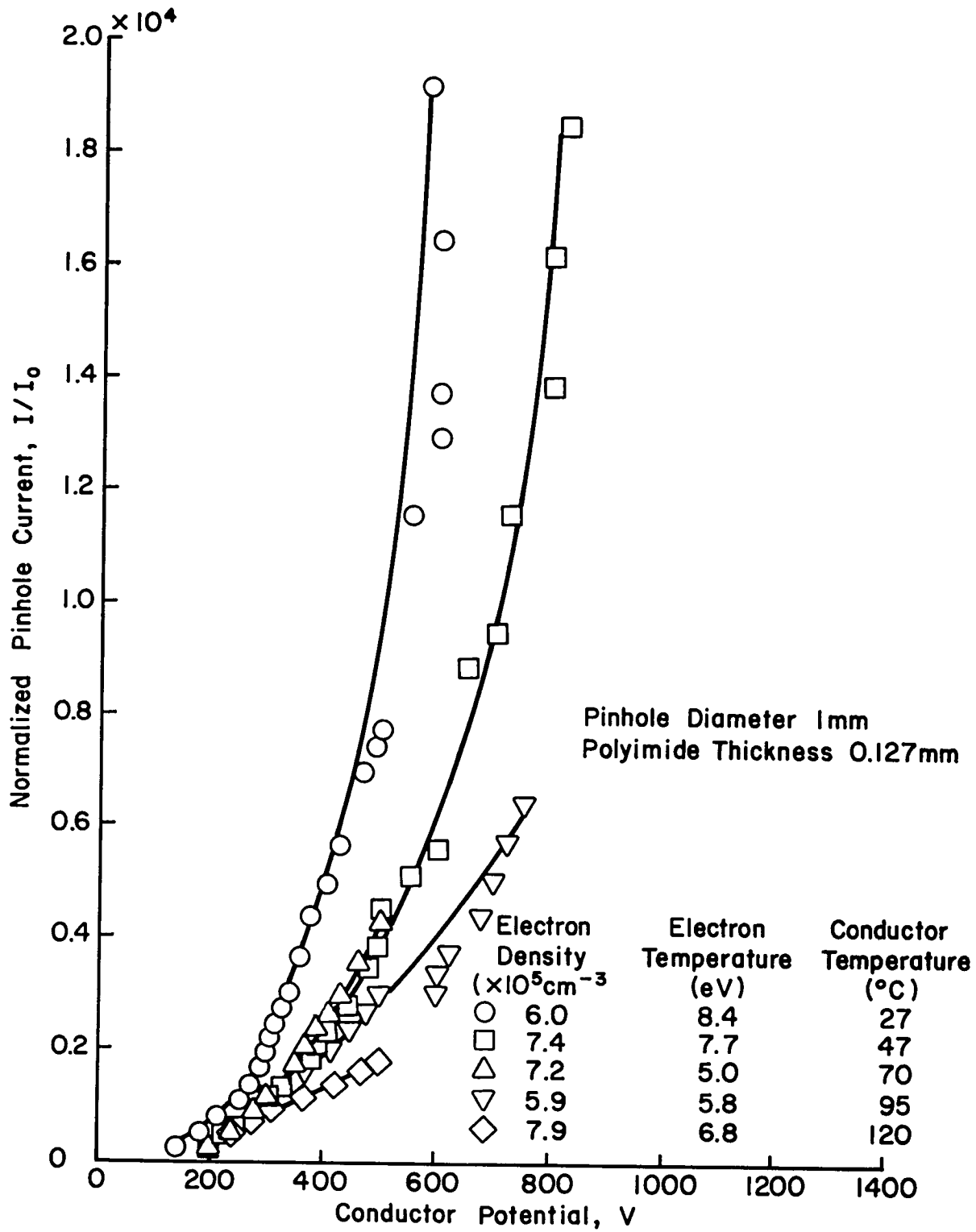


Fig. 3-4. The effect of conductor temperature on electron collection.

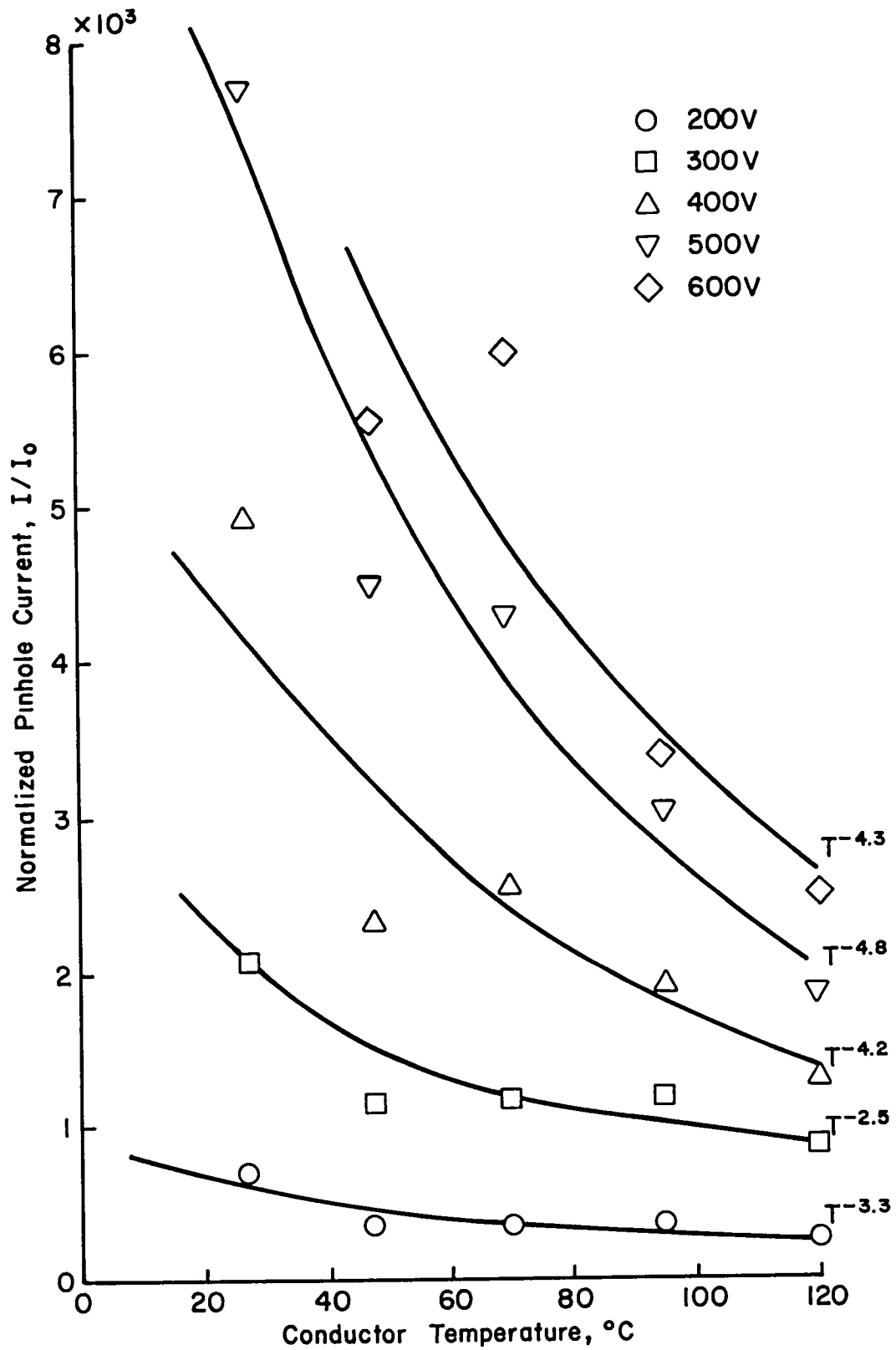


Fig. 3-5. Data of Fig. 3-4 plotted to show the effect of conductor temperature at constant conductor voltages. (Symbols shown were obtained by cross-plotting.)

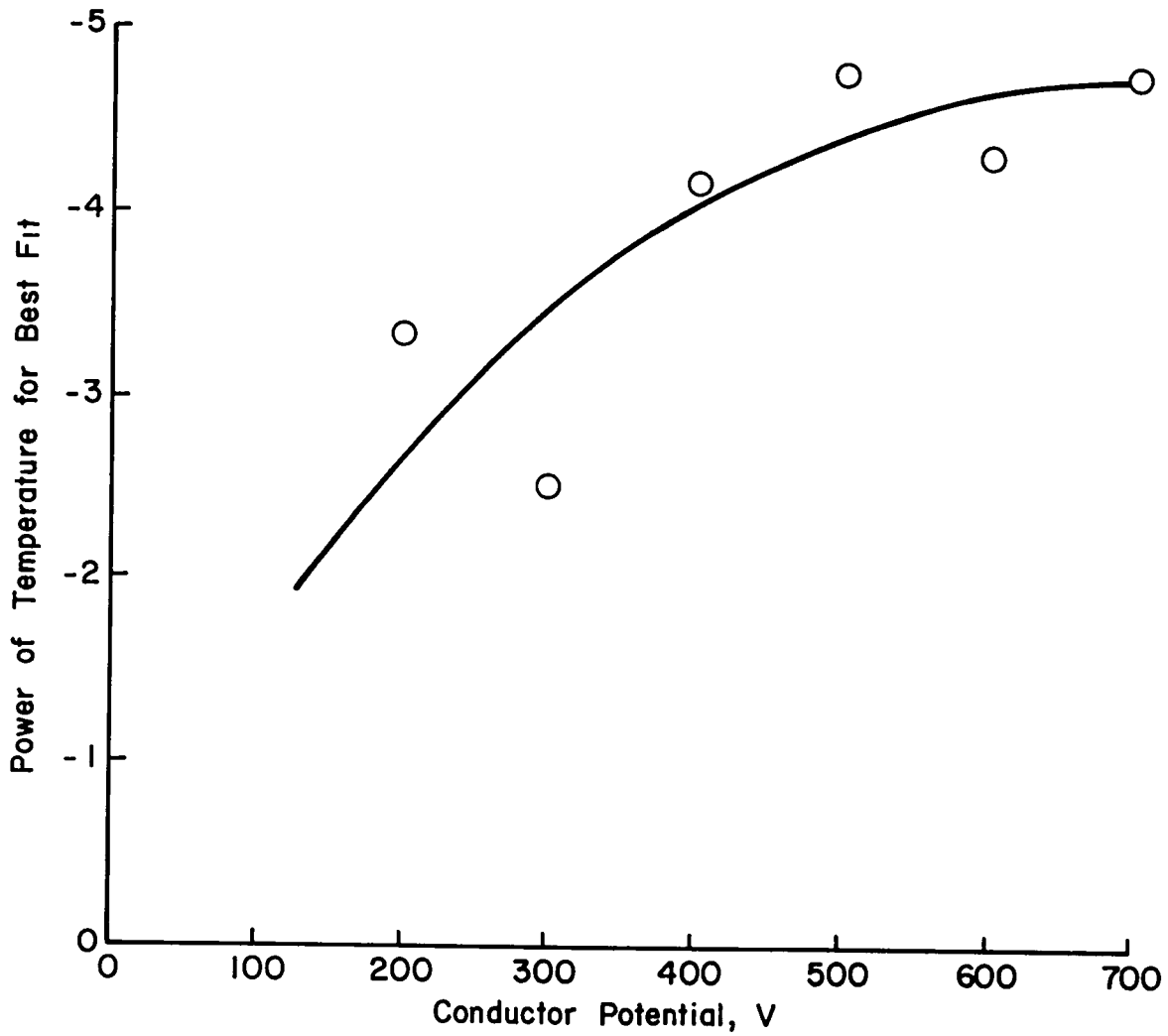


Fig. 3-6. Power of temperature variation for electron current as a function of conductor potential. (Symbols shown are best fits for the temperature variation.)

The lowering of collected current with roughened insulator surfaces that was reported earlier² also is in agreement with secondary electron emission as a major factor. That is, roughening a surface lowers the secondary electron emission coefficient.⁶

From the experimental observations at various conductor temperatures, then, it appears probable that secondary electron emission from insulators plays a major role in the collection of electron currents. Further, it appears that at least serial secondary electron events are involved in the conduction of an average electron to the conductor.*

Variation of Current Collection with Time. The data for a single configuration are typically obtained over a time of several minutes. It has been found that repeated tests showed decreased currents at the same voltages.² For the polyimide insulation used herein, this decrease in collected current could be prevented by roughening the inside of the hole in the insulator before testing it. An obvious question, and one of interest in space applications, is what happens during prolonged operation at a single conductor voltage.

The data of Fig. 3-7 were obtained at a conductor potential of 1000 V. The first current measurement gave a value of 700 μ A. From the usual short tests described elsewhere in this report a current of about 1500 μ A would be expected for the test conditions used.

It is clear from Fig. 3-7 that the collected current does not decrease continuously with time. The current shows instead occasional

*From Fig. 3-1 it should be evident that few electrons can pass from the plasma to the conductor without striking the insulator.

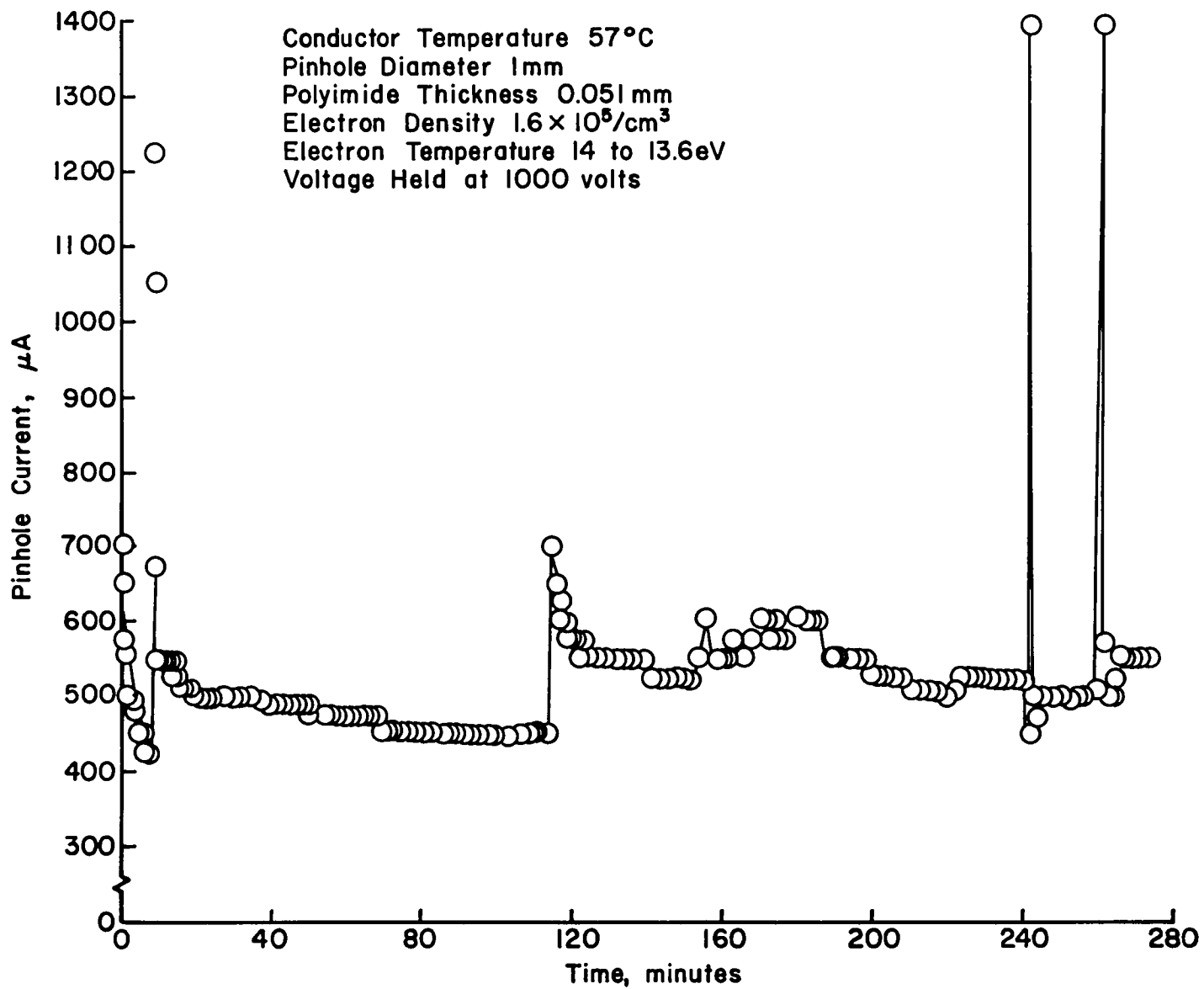
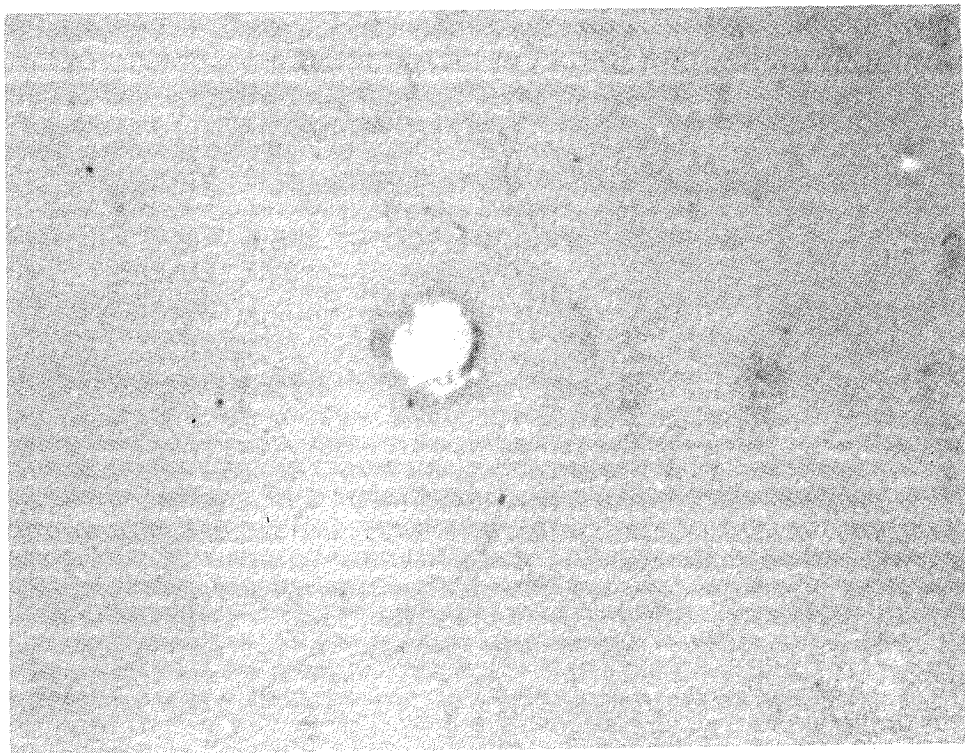
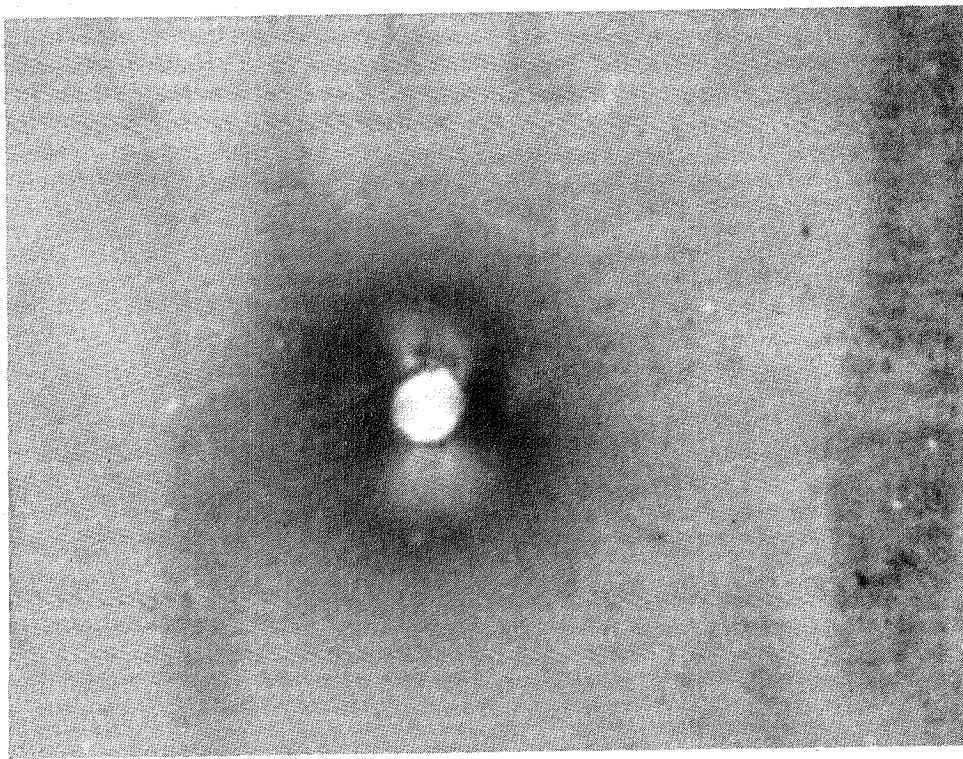


Fig. 3-7. Variation of electron current collection with collection time.



(a) Untested.



(b) After 375 min.

Fig. 3-8. Effect of current collection on insulator appearance.

transients of large magnitude, often followed by gradual decreases. These results have obvious significance to a spacecraft designer. One should expect a wide range of currents through a single hole, with no systematic variation with time, at least for the several hour duration investigated.

The polyimide insulator is darkened and beveled near the hole during a several hour test, as indicated in Fig. 3-8. The insulator sample used for Fig. 3-8(a) was not the same one that was used for the 375 min. test (Fig. 3-8(b)), but was quite similar in its initial appearance. The blackening and beveling of the sample in Fig. 3-8(b) supports the conclusion that, in time, the insulator is altered by the energetic bombardment of electrons.

Effect of Pinhole Size. Four pinhole diameters were investigated: 0.35, 0.52, 1.0, and 2.0 mm. This range of diameters gave an area range of over 30:1. This investigation also included polyimide thicknesses of 0.127 and 0.051 mm.

The data obtained with these different sized holes are presented in Figs. 3-9 and 3-10, with the data normalized in the same manner as described in the previous annual report.² That is, the collected electron currents were divided by the electron current that would result from random electron arrival at the same electron temperature and density, I_0 . As is evident in these figures, the data show a wide spread for the different hole sizes.

When a wide range of hole size is involved, a better normalization appears to be division by the random arrival electron current

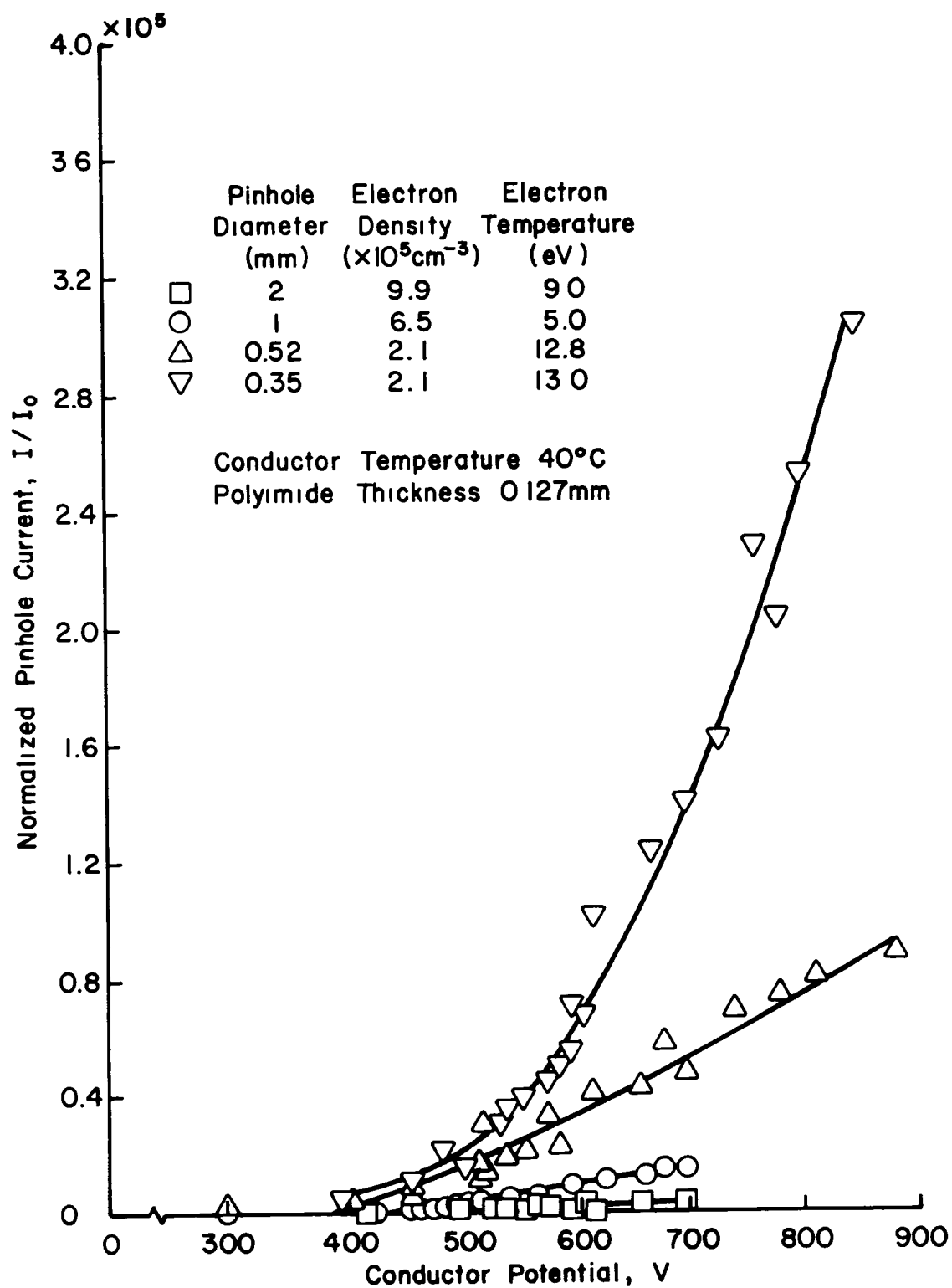


Fig. 3-9. Electron current collection characteristics for a range of hole sizes in 0.051 mm thick polyimide, normalized by I_0 .

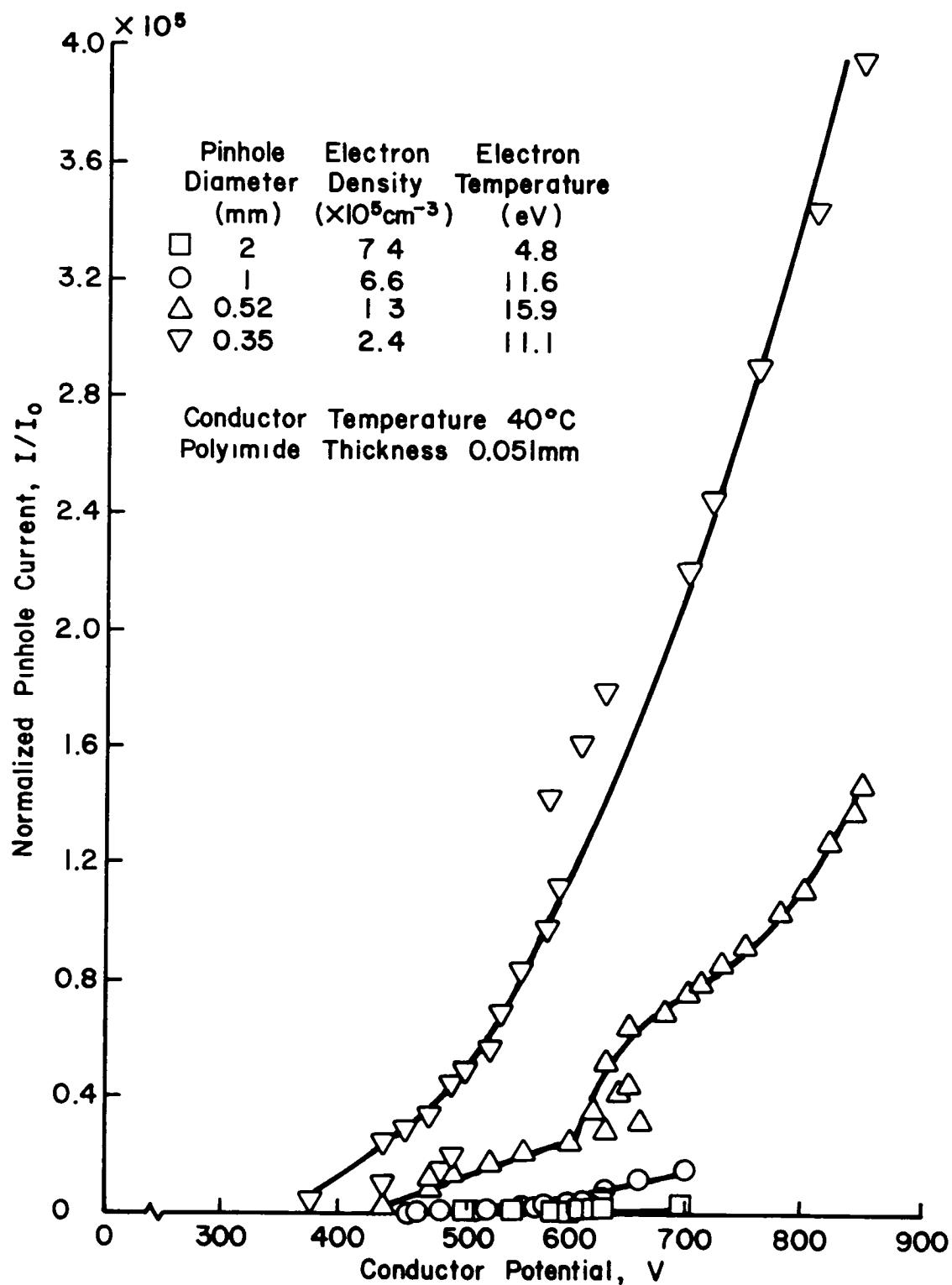


Fig. 3-10. Electron current collection characteristics for a range of hole sizes in 0.127 mm thick polyimide, normalized by I_0 .

density, j_o .^{*} The same data as shown in Figs. 3-9 and 3-10, normalized in this manner, are shown in Figs. 3-11 and 3-12. The normalization by j_o clearly gives a better correlation of data for different hole sizes than I_o .

The better correlation obtained with j_o results from the fact that the current at a given voltage is relatively insensitive to hole area. Physically, the quantity I/j_o represents the effective plasma area from which the random current density will provide the measured current. The exposed sample area is $1.44 \times 10^{-2} \text{ m}^2$. Most of the values of I/j_o shown correspond to areas less than the exposed sample area.

The plasma conditions under which the data of Figs. 3-9 through 3-12 were obtained should be emphasized, plasma conditions greatly different than those used should not be expected to give the same correlation.

Effect of Insulator Thickness. The electron current collection data shown in Figs. 3-11 and 3-12 are for two different thicknesses of the polyimide insulation. But the inclusion of all hole sizes on each figure makes it difficult to determine the effect of insulation thickness. These data are replotted in Fig. 3-13 through 3-16 to show the two different insulation thicknesses for a single hole size on each figure.

*The numerical value of j_o is given by

$$j_o = 2.68 \times 10^{-14} n T_e^{1/2}$$

where n is plasma density in m^{-3} and T_e is electron temperature in eV.

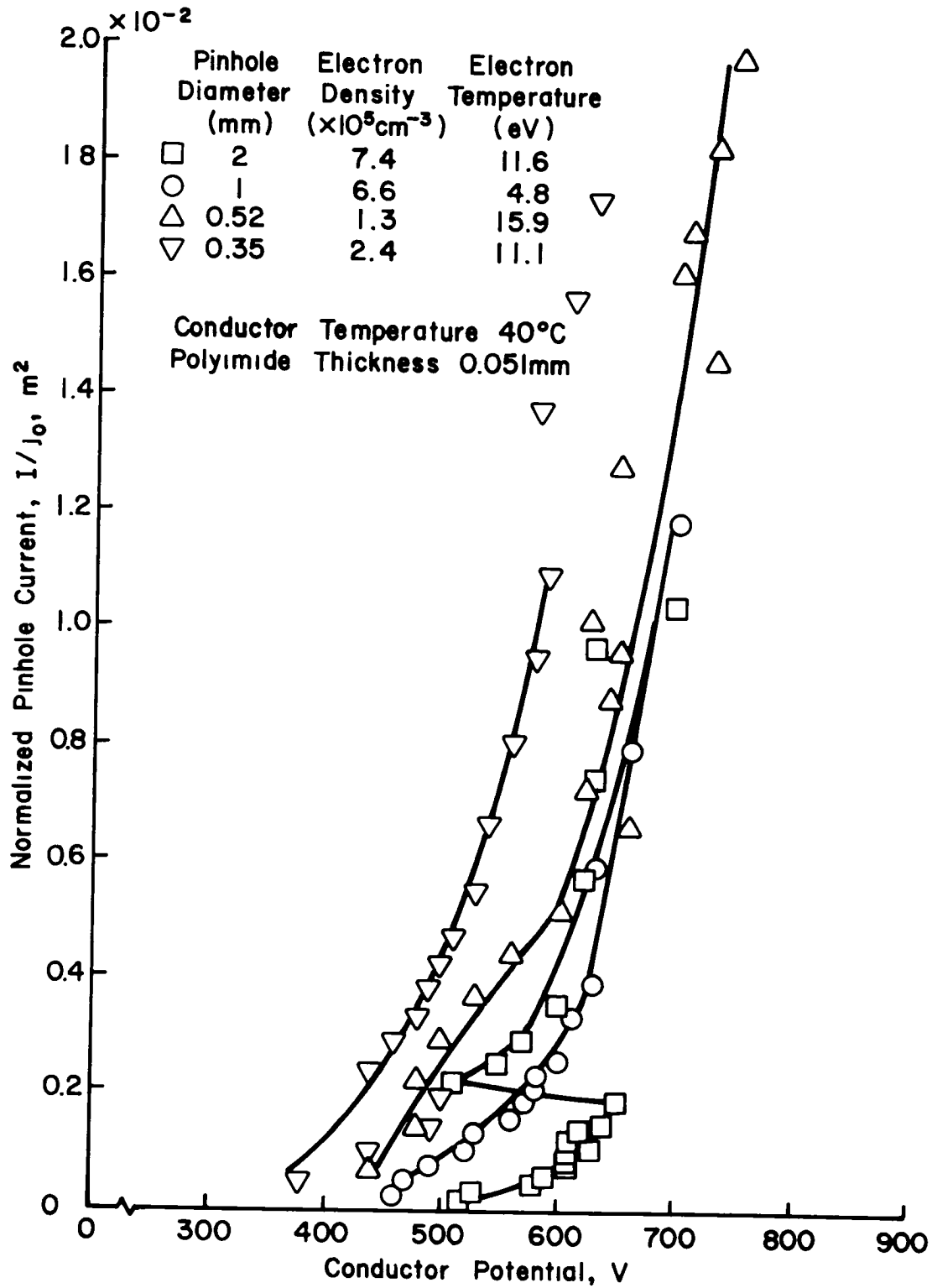


Fig. 3-11. Electron current collection characteristics for a range of hole sizes in 0.051 mm thick polyimide, normalized by j_0 .

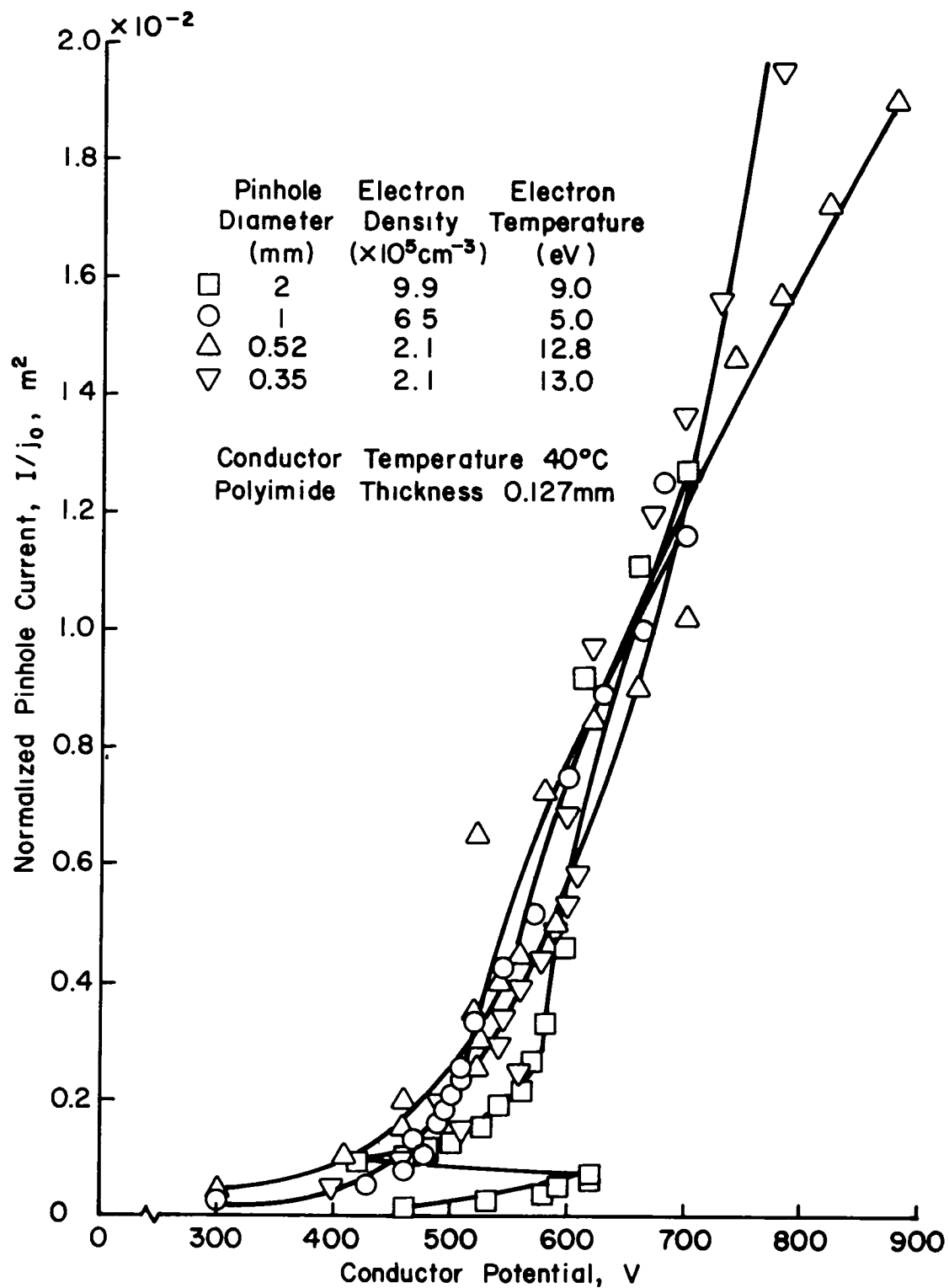


Fig. 3-12. Electron current collection characteristics for a range of hole sizes in 0.127 mm thick polyimide, normalized by j_0 .

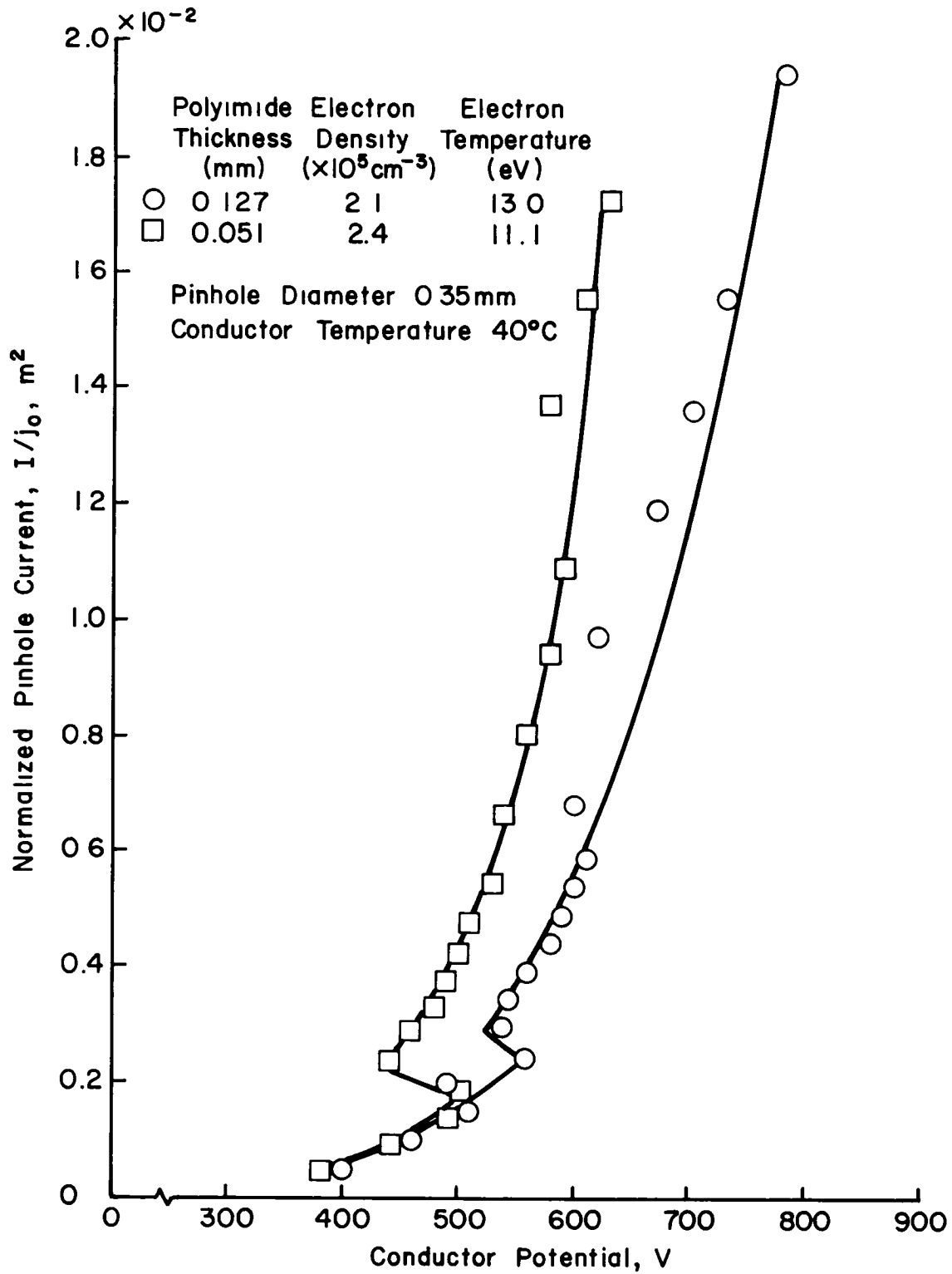


Fig. 3-13. Electron current collection characteristics for two insulation thicknesses and a hole diameter of 0.35 mm, normalized by j_0 .

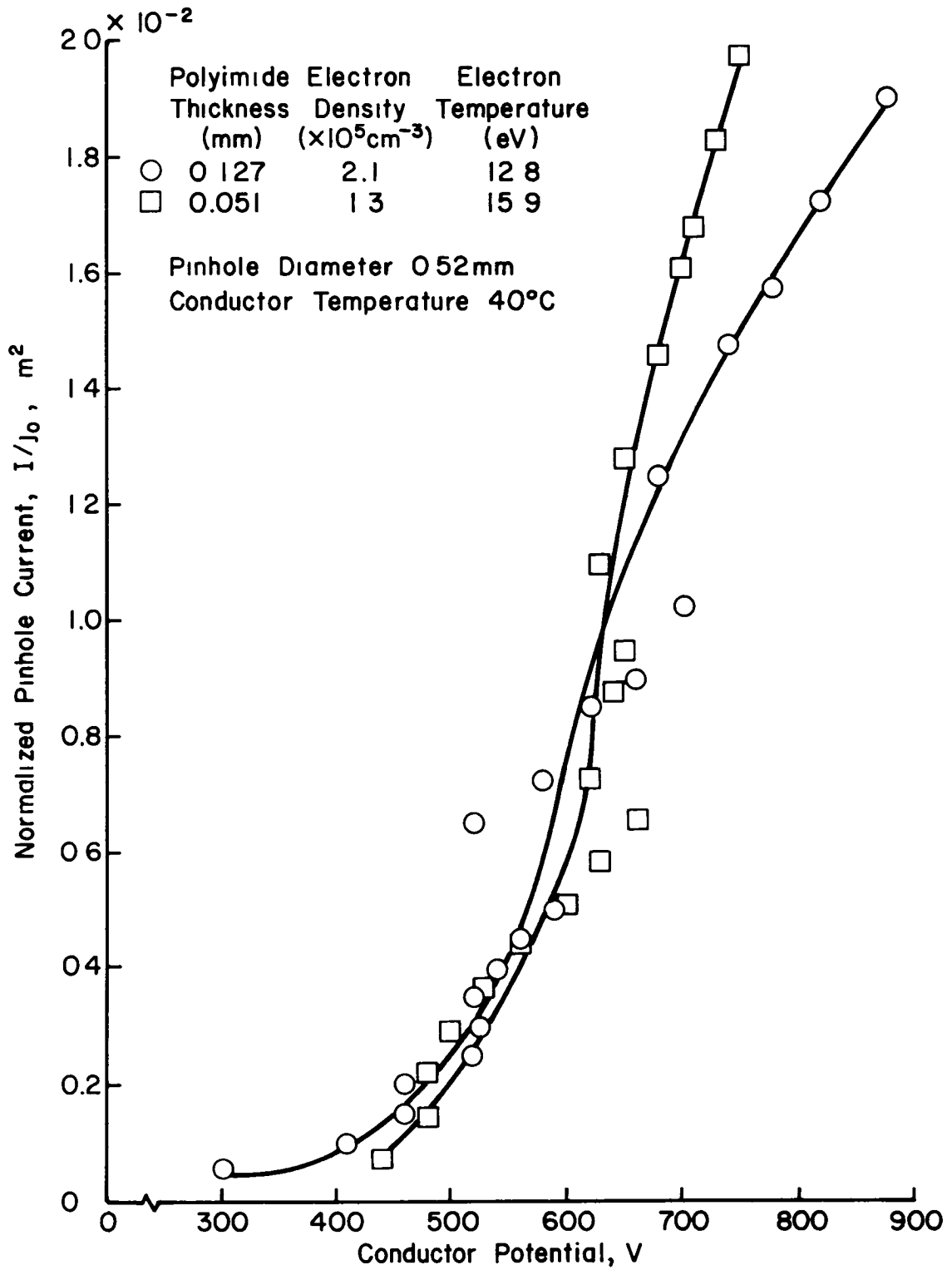


Fig. 3-14. Electron current collection characteristics for two insulation thicknesses and a hole diameter of 0.52 mm, normalized by J_0 .

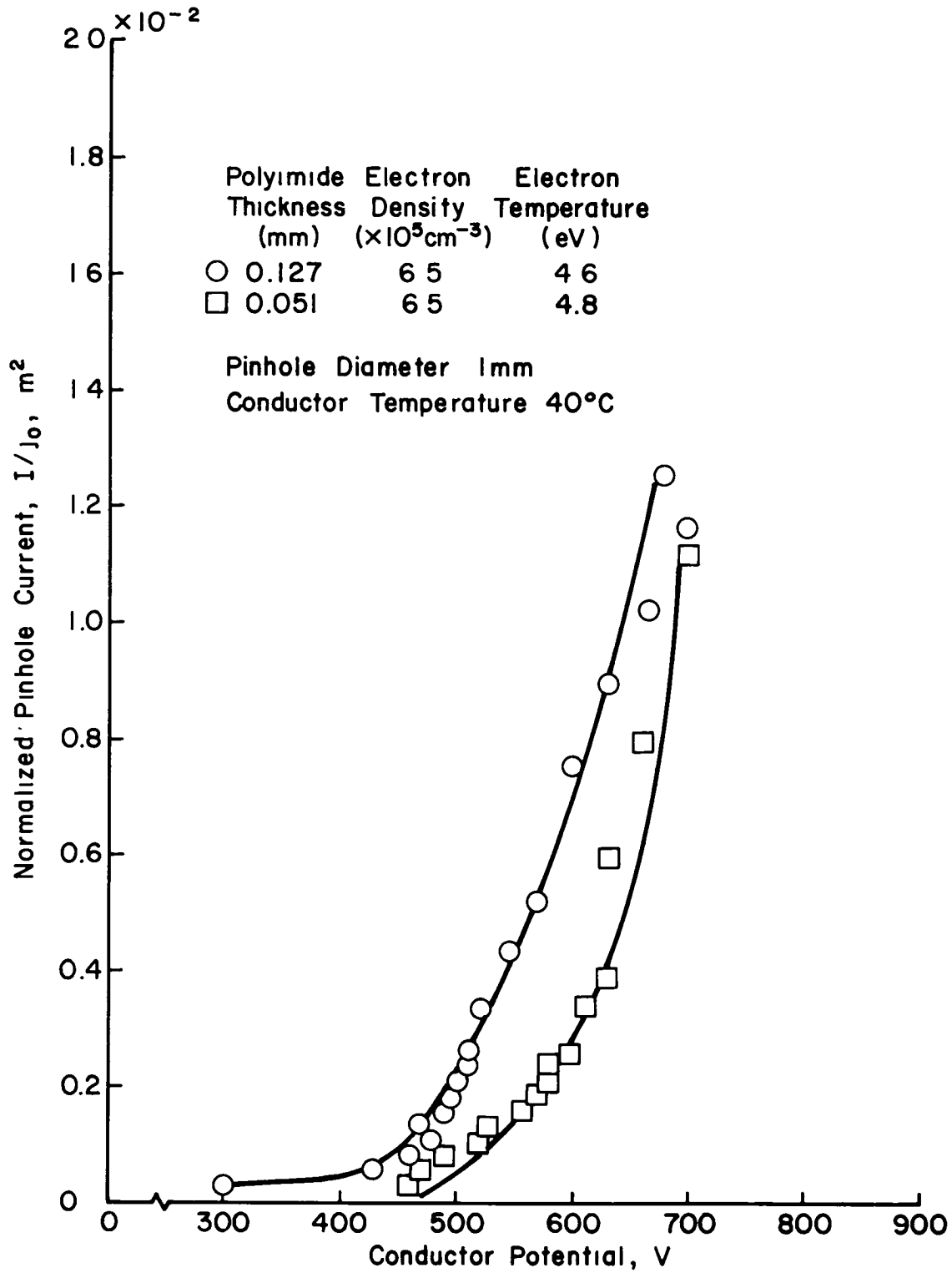


Fig. 3-15. Electron current collection characteristics for two insulation thicknesses and a hole diameter of 1.0 mm, normalized by j_0 .

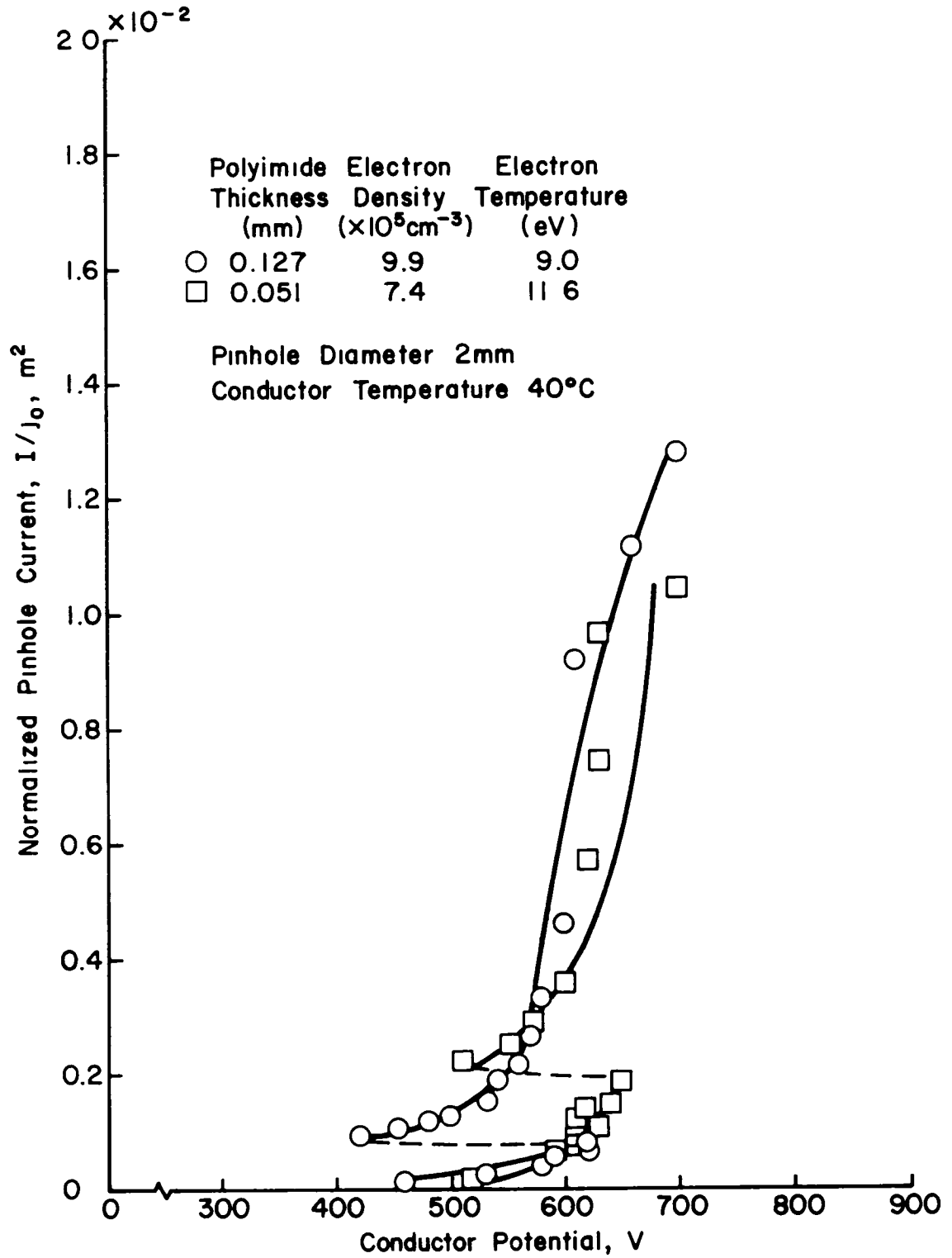


Fig. 3-16. Electron current collection characteristics for two insulation thicknesses and a hole diameter of 2.0 mm, normalized by j_0 .

For the insulation thicknesses used, insulation thickness has little effect on the electron current collection characteristics. Even the curve discontinuities evident in Figs. 3-13 and 3-16 are reproduced with the two thicknesses. The cause of these discontinuities is not entirely clear, but they are not associated with any large glows of the type described in the next section although occasionally small arcs can be seen in the pinhole in association with these sudden changes. The thickest insulator was still less than half the diameter of the smallest holes. It appears likely that thinner insulators would give the same results, as long as the insulator was not subject to direct breakdown at the applied voltages. If the insulation thickness approached the size of the hole diameter, insulation thickness could easily have an effect on the current collection characteristics.

High Current Measurements. Data were also obtained at higher current levels, up to 5 mA. Some of these data are shown in Fig. 3-17 for a 1 mm hole diameter, again normalized by j_o .

There are several breaks in the curve, as indicated in Fig. 3-17. These breaks are associated with a visible arc in the pinhole. At the higher current levels occurring after these breaks a glow was observed near the hole. This glow typically had the shape indicated in Fig. 3-18. The glow was centered about the pinhole with an arc still visible in the pinhole. The glow was also observed to change in intensity and extent with increasing current.

These breaks indicated possible changes in operating modes. Similar breaks were also indicated in Figs. 3-13 and 3-16, but no glows were visible, perhaps because the currents were a factor of several lower.

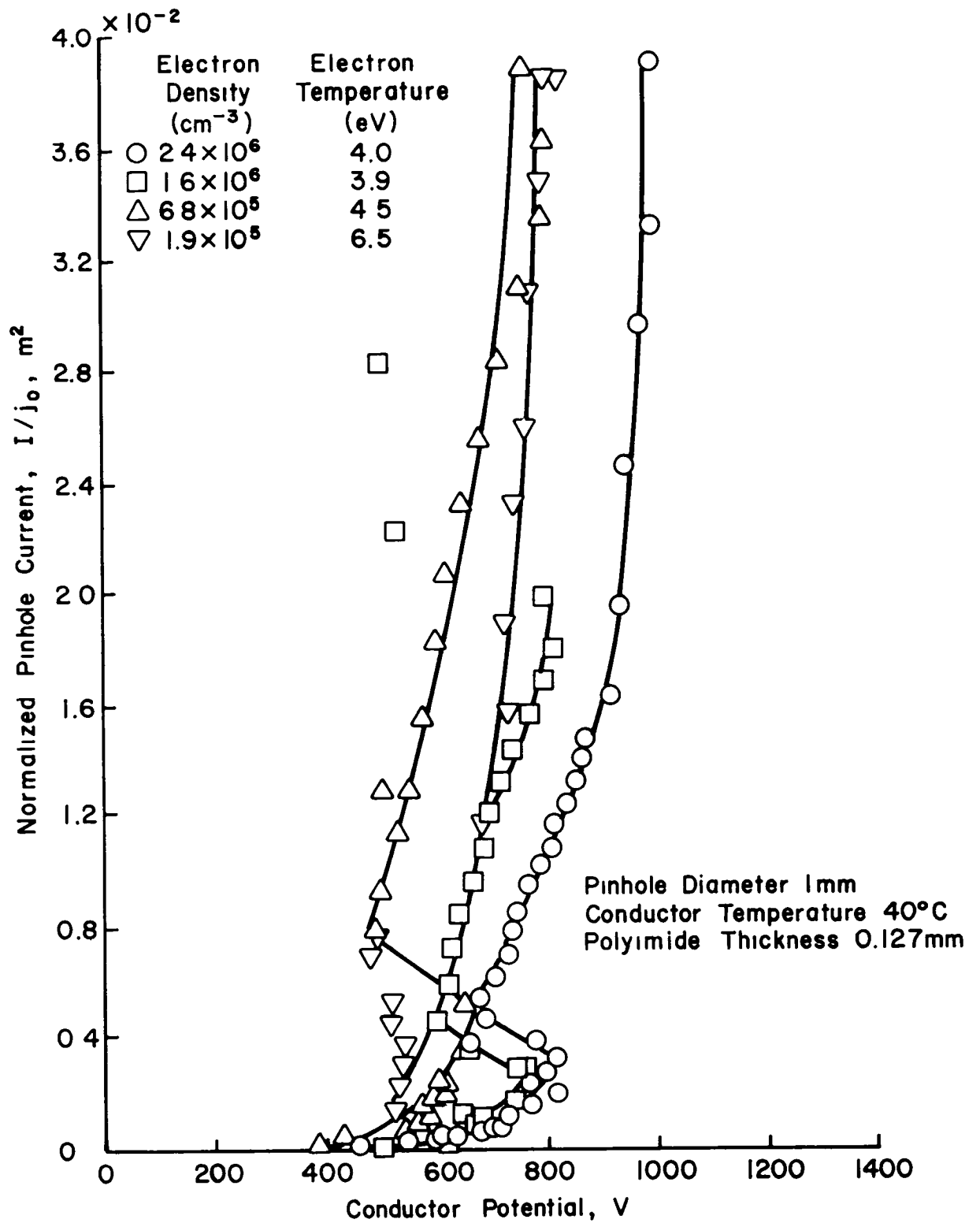
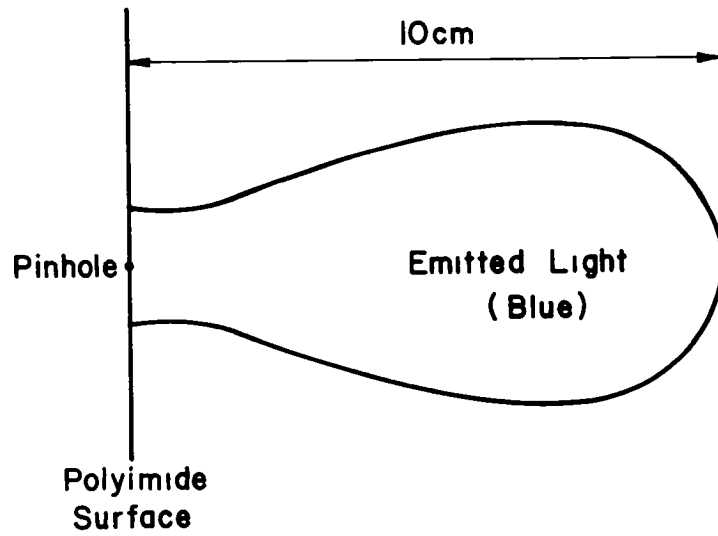
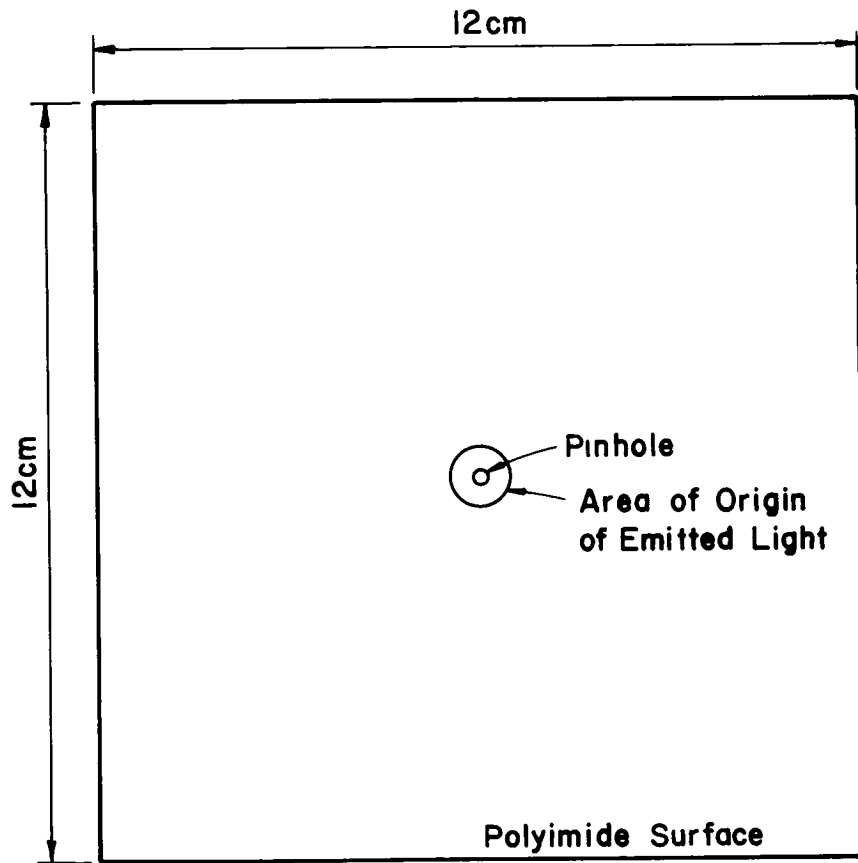


Fig. 3-17. Electron current collection characteristics extended to higher currents, normalized by j_0 .



Side View



Front View

Fig. 3-18. Glow observed near pinhole at higher electron collected currents.

The observation of glows raises some question as to the validity of the space simulation. The glows indicate de-excitation of atoms or molecules and/or electrons recombining with ionized atoms or molecules. If the atoms or molecules involved in the glow are from the insulator material, then the same process could be expected in space. If, on the other hand, the atoms or molecules were simply ambient background neutrals in the vacuum system, then the process would be expected to change at the lower neutral pressures found in space. The operating pressures herein (typically $\sim 2.0 \times 10^{-4}$ Torr) are low enough that most mean free paths exceed vacuum chamber dimensions. It is therefore quite possible that the space simulation is valid. But additional tests are required to establish this validity at high electron collection currents, when glows are visible.

Negative Bias - Ion Collection

Normalization. Because ion collection involves different charge carriers than electron collection, different normalization procedures should be used. The current density of ions arriving at a boundary is given by the Bohm current density (A/m^2),⁷

$$j_{Bohm} = n e (kT_e/m_i)^{1/2}, *$$

* A more convenient form is

$$j_{Bohm} = 2.48 \times 10^{-16} n T_e^{1/2}$$

with units the same as above, except T_e is electron temperature in eV.

where n is the electron/ion density, e is the electronic charge, k is Boltzmann's constant, T_e is the electron temperature, and m_i is the ion mass. The Bohm current, I_{Bohm} , is obtained by multiplying the Bohm current density by the hole area. These two parameters, j_{Bohm} and I_{Bohm} will be used for normalization. The gas used for the hollow cathode (argon) will be assumed for m_i .

Effect of Pinhole Size. Four hole diameters were tested: 2.0, 2.95, 4.1, and 4.99 mm. The selection of such large hole sizes were based largely on the small ion currents collected. Even with these large holes the measurements were frequently in the 10^{-8} A range.

The ion current collection data for the various hole sizes are shown in Figs. 3-19 and 3-20. In Fig. 3-19 the currents are corrected by j_{Bohm} , with a wide spread shown for the different hole sizes. When the data are corrected by I_{Bohm} , as shown in Fig. 3-20, this spread is greatly reduced. These results show that, unlike positive bias, hole area is an important parameter for negative bias and ion current collection. Also, for the voltage range covered, the ion current collected varied nearly linearly with negative voltage. Preliminary tests at larger negative voltages than -1000 V have shown large and variable current increases. The trends indicated in Figs. 3-19 and 3-20 should therefore not be extrapolated beyond the range shown.

Comparison with Planar Probe Theory. A comparison is shown in Fig. 3-21 between experimental ion current collection and planar probe theory (see the Appendix). The planar probe theory assumes that a grounded conductor surrounds the high-voltage circular probe area.³ Because an insulator replaced the conductor in the experiment, one should look for only approximate agreement.

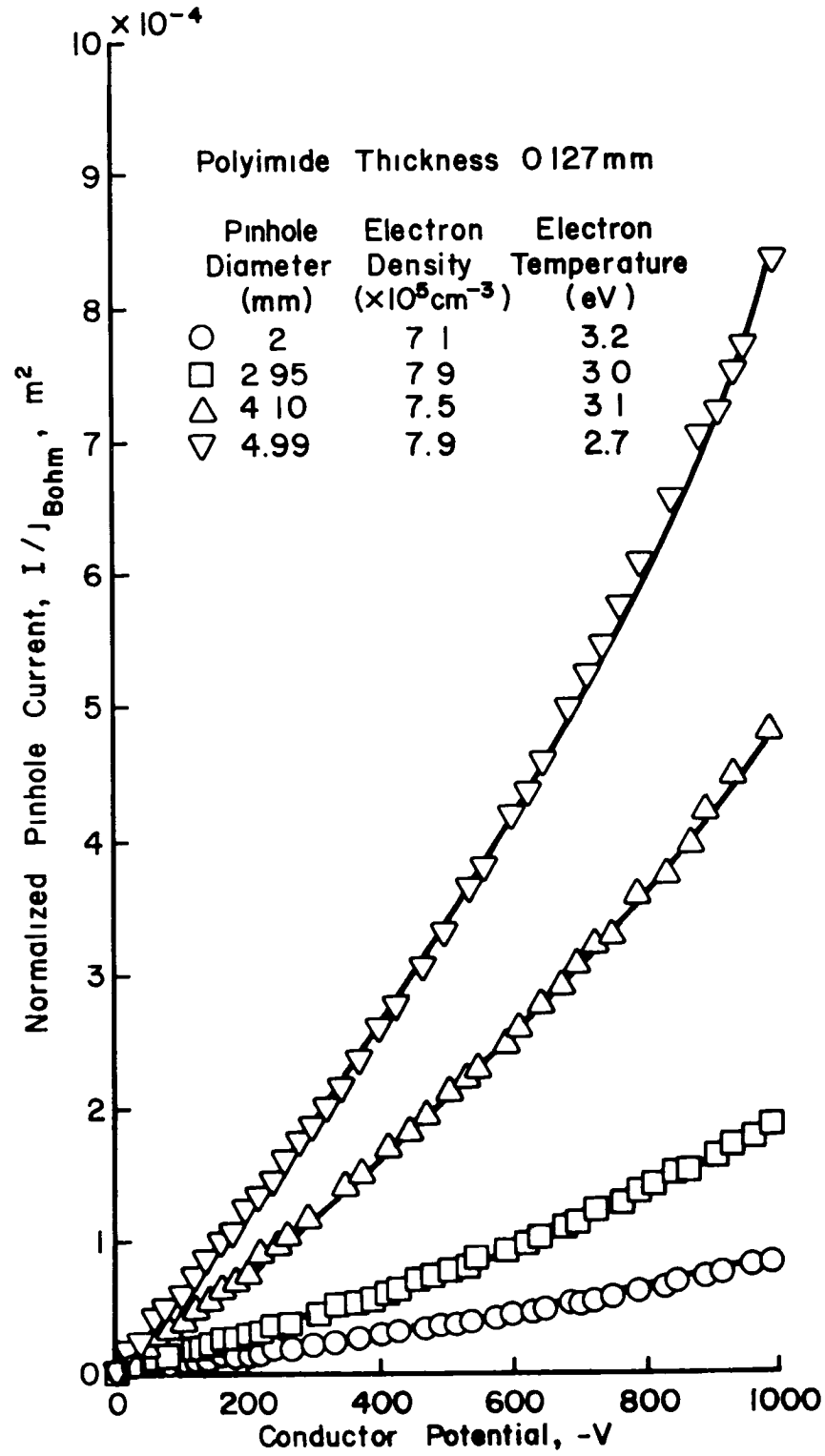


Fig. 3-19. Ion current collection characteristics for a range of hole sizes, normalized by j_{Bohm} .

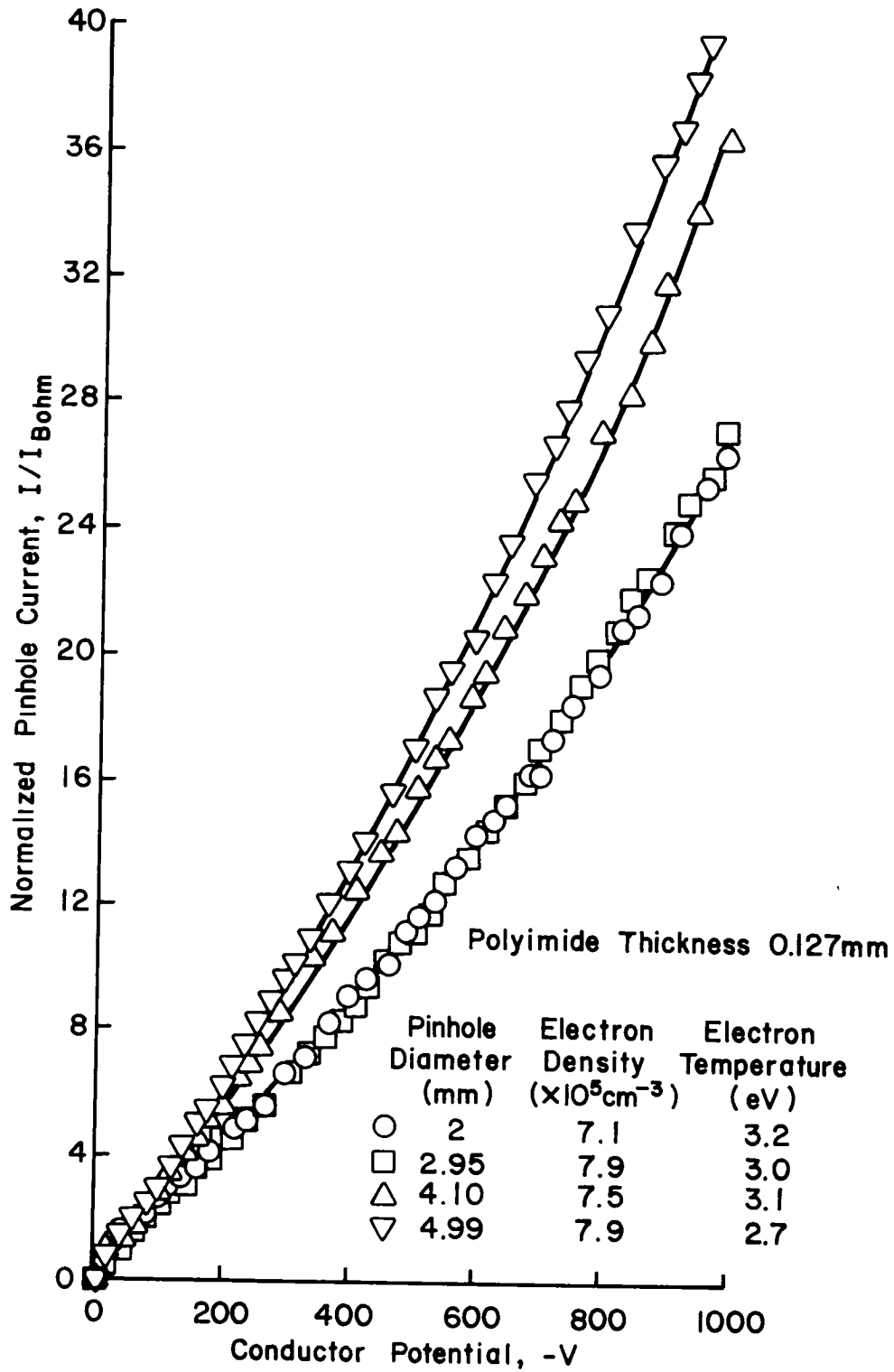


Fig. 3-20. Ion current collection characteristics for a range of hole sizes, normalized by I_{Bohm} .

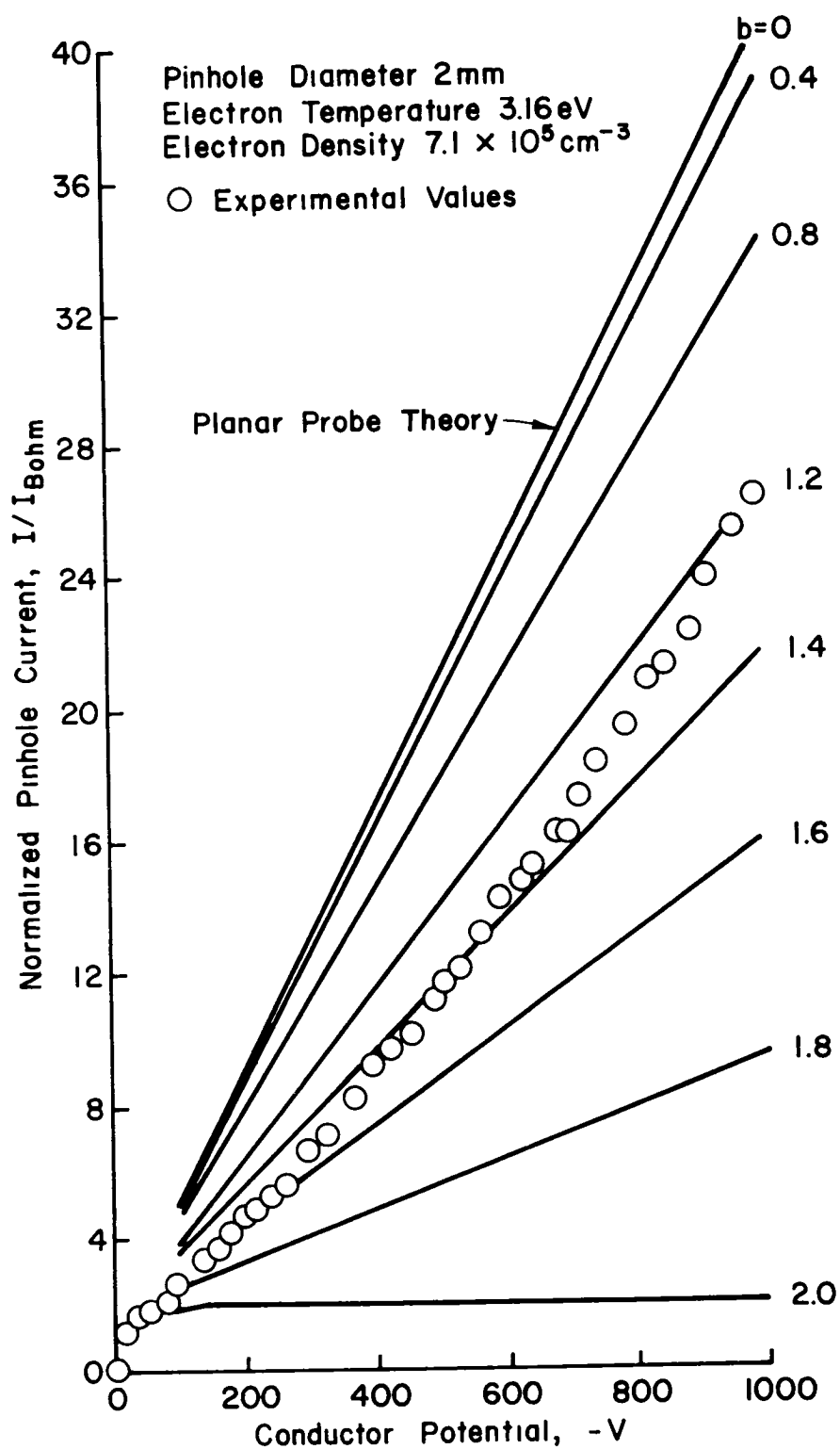


Fig. 3-21. Comparison of experimental ion current collection characteristics with planar probe theory (parameter b is an adjustable parameter of the probe theory - see the Appendix).

Hole size was not found to be a significant variable for electron collection in the $10^5 - 10^6 \text{ cm}^{-3}$ density range. As a result, normalization by random-arrival current density gave better data correlations than normalization by random-arrival current. Insulator thickness was also not a significant variable, although more affect on operation might be expected for thicknesses approaching the magnitude of the hole diameter.

Data were also obtained for ion collection (negative bias). For the 0-1000 V range of negative potential investigated, the results were qualitatively consistent with planar probe theory. It is therefore concluded that no current enhancing mechanism is necessary to explain the experimental results in this range. Preliminary data at more negative potentials indicate that conclusions may be different beyond -1000 V.

V. Appendix

MONOENERGETIC PLANAR PROBE THEORY

The probe theory most applicable to ion collection assumes monoenergetic energy to the charged particles. The geometry of the assumes probe is shown in Fig. A-1. In this theory, the probe potential (V_o) is referenced to the plasma potential, and the probe is flush with a surrounding conductor. In the sample holder, the insulator area surrounding the pinhole corresponds to the conductor surrounding the planar probe.

The equation describing the current collection of this planar probe is¹

$$I = I_o \left(1 + \frac{V_o}{E_o} - \frac{b^2}{4} \frac{V_o^2}{E_o(E_o + V_o)} \right)$$

where

$$I_o = I_{Bohm} = A_p n e \sqrt{\frac{k T_e}{m_i}} .$$

A_p is the pinhole area, n is the electron/ion density, e is the magnitude of the electronic charge, m_i is the mass of the ion, T_e is the electron temperature, k is the Boltzmann's constant, and E_o is the energy of the incoming ion. In this theory, E_o is defined by

$$j_o = \frac{en}{4} \sqrt{\frac{2E_o}{m_i}}$$

Since $j_o = j_{Bohm}$ for ion collection, then

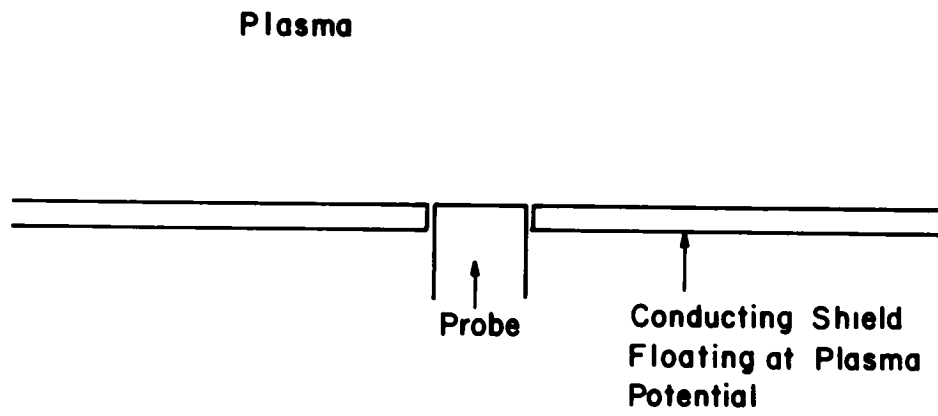


Fig. A-1. Geometry of planar probe.

$$E_o = 8 k T_e.$$

The parameter b is adjustable and is related to the trajectories of the incoming ions. The parameter b can range from 0 to 2.

VI. REFERENCES

Section I

1. D. J. Santeler, D. H. Holkeboer, D. W. Jones, and F. Pagano, "Vacuum Technology and Space Simulation," NASA Special Publication SP-105, pp. 33-40, 1967.
2. J. H. Wolfe, in "Solar Wind" (edited by C. P. Sonett, P. J. Coleman, Jr., and J. M. Wilcox), NASA Special Publication SP-308, pp. 170-201, 1972.
3. C. R. Chappell, Rev. of Geophysics and Space Physics, Vol. 10, pp. 951-979, Nov. 1972.
4. R. K. Cole, H. S. Ogawa, and J. M. Sellen, Jr., AIAA Paper No. 69-262 (1969).
5. N. T. Grier and D. J. McKinzie, AIAA Paper No. 69-262 (1969).
6. J. R. Bayless, B. G. Herron, and J. D. Worden, AIAA Paper No. 72-443 (1972).
7. N. T. Grier and S. Domitz, NASA Tech. Note TN D-8111 (1975).
8. K. L. Kennerud, NASA Contractor Report CR-121280 (1974).
9. H. R. Kaufman and R. S. Robinson, "Interaction of High Voltage Surfaces with the Space Plasma," NASA Contr. Rep. CR-159731, May 1979.

Section II

1. H. R. Kaufman and R. S. Robinson, "Interaction of High Voltage Surfaces with the Space Plasma," NASA Contr. Rep. CR-159731, May 1979.

Section III

1. Martin A. Uman, Introduction to Plasma Physics, New York, McGraw Hill, Inc., pp. 19-22, 1964.
2. H. R. Kaufman and R. S. Robinson, "Interaction of High Voltage Surfaces with the Space Plasma," NASA Contr. Rep. CR-159731, May 1979.
3. L. W. Parker and E. C. Whipple, "Theory of a Satellite Electrostatic Probe," Annals of Physics 44, pp. 126-167 (1967).

4. F. F. Chen, "Electric Probes," Plasma Diagnostic Techniques, Huddleston, R. H. and Leonard, S. L., editors, Academic Press, New York, pp. 113-135 (1965).
5. D. J. Gibbons, "Secondary Electron Emission," in Handbook of Vacuum Physics, Vol. 2, Physical Electronics (A. H. Beck, ed.), Pergamon Press, Glasgow, Scotland, pp. 301-395 (1966).
6. S. F. Rashkovski, "Secondary Emission from Rough Surfaces," Radio Engng. Electron Physics 3, pp. 97-117 (1958).
7. Francis F. Chen, Introduction to Plasma Physics, New York, Plenum Press, pp. 246-247, 1977.

Section IV

1. H. R. Kaufman and R. S. Robinson, "Interaction of High Voltage Surfaces with the Space Plasma," NASA Contr. Rep. CR-159731, May 1979.

Section V

1. L. W. Parker and E. C. Whipple, "Theory of a Satellite Electrostatic Probe," Annals of Physics 44, pp. 126-167 (1967).

DISTRIBUTION LIST

	<u>No. of Copies</u>
National Aeronautics and Space Administration Washington, DC 20546	
Attn: RPE/Mr. Wayne Hudson	1
Mr. Daniel H. Herman, Code SL	1
National Aeronautics and Space Administration Lewis Research Center 21000 Brookpark Road Cleveland, OH 44135	
Attn: Research Support Procurement Section	
Mr. L. Light, MS 500-306	1
Technology Utilization Office, MS 3-19	1
Report Control Office, MS 5-5	1
Library, MS 60-3	2
N. T. Musial, MS 600-113	1
Spacecraft Propulsion & Power Division, MS 501-7	
Dr. F. Teren	1
Mr. R. Finke	1
Mr. D. Byers	1
Mr. B. Banks	1
Mr. N. Grier	1
Mr. F. Terdan	20
Mr. W. Kerslake	1
Mr. V. Rawlin	1
Mr. M. Mirtich	1
Chief Scientist, MS 3-12	1
Dr. M. Goldstein	1
National Aeronautics and Space Administration Marshall Space Flight Center Huntsville, AL 35812	
Attn: Mr. Jerry P. Hethcoate	1
Mr. John Harlow	1
NASA Scientific and Technical Information Facility P. O. Box 8757 Baltimore/Washington International Airport Baltimore, MD 21240	40
Case Western Reserve University 10900 Euclid Avenue Cleveland, OH 44106	
Attn: Dr. Eli Reshotko	1
Royal Aircraft Establishment Space Department Farnborough, Hants, ENGLAND	
Attn: Dr. D. G. Fearn	1

NASA JSC	
Houston, TX 77058	
Attn: Mr. H. Davis	1
United Kingdom Atomic Energy Authority	
Culham Laboratory	
Abingdon, Berkshire, ENGLAND	1
Attn: Dr. P. J. Harbour	1
Dr. M. F. A. Harrison	1
Dr. T. S. Green	1
National Aeronautics and Space Administration	
Goddard Space Flight Center	
Greenbelt, MD 20771	1
Attn: Mr. W. Isley, Code 734	1
Mr. A. A. Yetman	1
Dr. D. H. Suddeth	1
Comsat Laboratories	
P. O. Box 115	
Clarksburg, MD 20734	1
Attn: Mr. B. Free	1
Mr. O. Revesz	
Rocket Propulsion Laboratory	
Edwards AFB, CA 93523	1
Attn: LKDA/Mr. Tom Waddell	1
LKDH/Dr. R. Vondra	
DFVLR - Institut für Plasmadynamik	
Technische Universität Stuttgart	
7 Stuttgart-Vaihingen	
Allmandstr 124	
WEST GERMANY	1
Attn: Dr. G. Krülle	
Giessen University	
1st Institute of Physics	
Geissen, WEST GERMANY	1
Attn: Professor H. W. Loeb	
Jet Propulsion Laboratory	
4800 Oak Grove Drive	
Pasadena, CA 91102	1
Attn: Dr. Kenneth Atkins	1
Technical Library	1
Mr. Eugene Pawlik	1
Dr. Graeme Aston	1
Dr. Kevin Rudolph	1

Electro-Optical Systems, Inc.	
300 North Halstead	
Pasadena, CA 91107	
Attn: Mr. R. Worlock	1
Mr. E. James	1
Mr. W. Ramsey	1
Boeing Aerospace Company	
P. O. Box 3999	
Seattle, WA 98124	
Attn: Mr. Donald Grim	1
Mr. Russel Dod	1
Lockheed Missiles and Space Company	
Sunnyvale, CA 94088	
Attn: Dr. William L. Owens	
Propulsion Systems, Dept. 62-13	1
Mr. Carl Rudey	1
Fairchild Republic Company	
Farmingdale, NY 11735	
Attn: Dr. William Guman	1
COMSAT Corporation	
950 L'Enfant Plaza S.W.	
Washington, DC 20024	
Attn: Mr. Sidney O. Metzger	1
Electrotechnical Laboratory	
Tahashi Branch	
5-4-1 Mukodai-Machi, Tanashi-Shi	
Tokyo, JAPAN	
Attn: Dr. Katsuva Nakayama	1
Office of Assistant for Study Support	
Kirtland Air Force Base	
Albuquerque, NM 87117	
Attn: Dr. Calvin W. Thomas OAS Ge	1
Dr. Berhart Eber OAS Ge	1
Bell Laboratories	
600 Mountain Avenue	
Murray Hill, NJ 07974	
Attn: Dr. Edward G. Spencer	1
Dr. Paul H. Schmidt	1
Massachusetts Institute of Technology	
Lincoln Laboratory	
P. O. Box 73	
Lexington, MA 02173	
Attn: Dr. H. I. Smith	1

Sandia Laboratories
 Mail Code 5742
 Albuquerque, NM 87115
 Attn: Mr. Ralph R. Peters 1

TRW, Inc.
 TRW Systems
 One Space Park
 Redondo Beach, CA 90278
 Attn: Dr. M. Huberman 1
 Mr. H. Ogawa 1
 Mr. S. Zafran 1

National Aeronautics and Space Administration
 Ames Research Center
 Moffett Field, CA 94035
 Attn: Technical Library 1

National Aeronautics and Space Administration
 Langley Research Center
 Langley Field Station
 Hampton, VA 23365
 Attn: Technical Library 1

Hughes Research Laboratories
 3011 Malibu Canyon Road
 Malibu, CA 90265
 Attn: Dr. J. Hyman 1
 Mr. J. H. Molitor 1
 Dr. R. L. Poeschel 1
 Mr. R. Vahrenkamp 1
 Dr. John R. Beattie 1
 Dr. W. S. Williamson 1

United States Air Force
 Office of Scientific Research
 Washington, DC 20025
 Attn: Mr. M. Slawsky 1

Princeton University
 Princeton, NJ 08540
 Attn: Dean R. G. Jahn 1
 Dr. K. E. Clark 1

Joint Institute for Laboratory Astrophysics
 University of Colorado
 Boulder, CO 80302
 Attn: Dr. Gordon H. Dunn 1

Service du Confinement des Plasma
 Centre d'Etudes Nucléaires - F.A.R.
 B. P. 6
 92260 Fontenay-aux-Roses
 FRANCE
 Attn: Dr. J. F. Bonal

1

International Business Machines Corporation
 Thomas J. Watson Research Center
 P. O. Box 218
 Yorktown Heights, NY 10598
 Attn: Dr. Jerome J. Cuomo
 Dr. James M. E. Harper

1

1

IBM East Fishkill
 D/42K, Bldg. 300-40F
 Hopewell Junction, NY 12533
 Attn: Dr. Charles M. McKenna

1

DFVLR-Forschungszentrum Braunschweig
 Inst. A, Flughafen
 3300 Braunschweig
 WEST GERMANY
 Attn: Dr. H. A. W. Bessling

1

Ion Beam Equipment, Inc.
 P. O. Box 0
 Norwood, NJ 07648
 Attn: Dr. W. Laznovsky

1

Optic Electronics Corporation
 11477 Pagemill Road
 Dallas, TX 75243
 Attn: Bill Hermann, Jr.

1

Circuits Processing Apparatus, Inc.
 725 Kifer Road
 Sunnyvale, CA 94086
 Attn: Spencer R. Wilder

1

Ion Tech, Inc.
 1807 E. Mulberry
 P. O. Box 1388
 Fort Collins, CO 80522
 Attn: Dr. Gerald C. Isaacson

1

Physicon Corporation
 221 Mt. Auburn Street
 Cambridge, MA 02138
 Attn: H. von Zweck

1

Commonwealth Scientific Corporation
500 Pendleton Street
Alexandria, VA 22314
Attn: George R. Thompson

1

Veeco Instruments Inc.
Terminal Drive
Plainview, NY 11803
Attn: Norman Williams

1

CVC Products
525 Lee Road
P. O. Box 1886
Rochester, N.Y. 14603
Attn: Mr. Georg F. Garfield, Jr.

1

End of Document